ISTITUTO NAZIONALE DI FISICA NUCLEARE

Sezione di Milano

INFN/TC-08/5
September 29, 2008

THERMAL CONDUCTIVITY MEASUREMENTS AT CRYOGENIC TEMPERATURES: HARDWARE AND SOFTWARE APPARATUS

Antonio Paccalini, Giancesare Rivoltella and Giovanni Volpini

INFN- Sezione di Milano- LASA e Dip. di Fisica-Università degli Studi di Milano, Via F.lli Cervi 201, I-20090 Segrate(MI), Italy

Abstract

An apparatus to measure the thermal conductivity of bulk samples at cryogenic temperatures is in use at LASA Laboratory since some years.

The Magnex Scientific Ltd cryostat and the inner mechanical system realized at LASA, have maintained good performances during the time. On the contrary, the electrical connections have been damaged by the thermal cycles experienced, for this reason they have been replaced. The realization of the thermal sensors, AuFe (0.07% at.w.)-Cromel P thermocouples (TC), has been improved and standardized.

A new electronic system, h/w and s/w, has been realized. The temperatures are acquired by a nanovoltmeter, while the measure parameters (pressures, cryogenic levels, etc) are acquired by a precision multiplexer. The acquisition, the storage and the readout of the data are managed in real time by LabView 8.5.

The reliability of the measures and the quantity of the data have allowed a deeper study of instrumental phenomena as, for instance, the capacitive effect of the nitrogen level probe on the TC voltage and the relationship between the different thermal zero levels and the physical conditions of the apparatus.

PACS.: 72.15 Cz, 65.60. +a

Published by ***SIS–Pubblicazioni***
Laboratori Nazionali di Frascati

1 INTRODUCTION

The knowledge of the thermal conductivity inside a superconducting winding has a key role in the study of the quench propagation [1].

In an adiabatic magnet the transverse propagation, turn to turn and layer to layer, is an important mechanism of the quench propagation. In this condition the heat diffuses through the insulator, while in the longitudinal propagation, along the cable, the heat propagates through the metal stabilizer.

The thermal conductivities, longitudinal (λ_l) and transverse (λ_t), are connected to the quench speed propagation and therefore the knowledge of such parameters is fundamental to guarantee the magnet safety in case of quench.

The λ_l can easily be computed as a function of temperature and magnetic field. Considering negligible the heat conduction in the insulator, the main contribution is given by the metals, the copper matrix primarily: λ_l can be calculated by considering the thermal conductance of the cable components in parallel.

The evaluation of transverse conductivity is not easy instead. A serial-parallel conductivity model is not reliable owing to cable constructive complexity: the superconductive filaments are embedded in a CuSn matrix and thin barriers, for instance in Ta, are realized to insulate it. A multistrand cable complicates the evaluation of λ_t.

From this we have the necessity of an experimental apparatus for the thermal conductivity measurement, both for coil blocks (samples derived from superconductive cables) and for composite materials used in the cryomagnetic apparatus.

The LASA conductimeter has been designed to measure the thermal conductivity using the stationary method of the axial heat flux, based on the Fourier-Biot law, where every value of λ_t is related to the mean temperature of a sample.

The report presents the system of measure, its design and operation details. The mechanics of the apparatus has substantially remained the same one described in reports [1], [8] and thesis of degree [2], while the acquisition hardware and software have been completely rebuilt. Furthermore the new approach in the data analysis allows the study of the physical limits of the system and a comparison among experimental and theoretical data.

2 DESCRIPTION OF THE APPARATUS OF MEASURE

2.1 Mechanics and electronics

The apparatus is composed by a dewar built by the Magnex Scientific Ltd, in which the system of measure is located.

Fig.1 shows the cryostat and the apparatus. Fig.2 shows the complete measure system.

Two cylindrical blocks of copper OHFC (Oxygen Free High Conductivity) are the heat sinks; they embrace the sample by a pressing system. The cold heat sink, placed above the sample, is at the cryogenic fluid temperature. The bottom plate, the hot heat source, generates a heat flow into the sample from the lower to upper part.

The pressing system is composed by four stainless steel rods with loading springs, it pushes a disk of G11 (Glass-epoxy laminate), the pressing plate, to enhance the thermal contact between the sample and the heat sinks. The thermal resistance is reduced by a thin layer of Cryo-Con®, cryogenic thermal conductive grease whose thermal conductivity is of 0.1 W/m·K at 4.2 K.

On the cold sink is brazed a copper disk where both the leads of every thermocouple are soldered. This type of electrical connection, for the empirical law of the intermediate metals, constitutes the thermal reference junction, or isothermal block (i.b.); if the i.b. temperature remains constant, the TCs can be connected with normal copper wires from the i.b., to the outside without effect on the emf [3].

The thermal conductimeter is closed in a vacuum chamber and an Indium seal guarantees the tightness. Three vacuum connectors and three pipes (the pumping, the vacuum probe and the He gas inlet) are positioned on the upper flange.

The temperature is measured by eight AuFe (0.07% at.w.)-Cromel P thermocouples: six positioned on the sample, two on the thermal sinks.

The acquisition system is schematized in Fig. 3.

The range of the thermocouples emf, normalized to 4.215 K according to the cryogenic fluid of reference, reaches 1.3 mV at 110 K.

The thermocouples sensitivity in the range 4÷100 K is 10-20 μV/K, this means that the acquisition instrument must have a resolution of 10 nV to measure 1 mK of ΔT. It becomes therefore essential the use of a nanovoltmeter combined to a low noise scanner: the NanoVoltmeter HP34420A and the nV Scanner Keithley 7001. These measures are made in a noisy environment with industrial power apparatuses (pumps, power supply, and fan heater), consequently 100 nV is the overall pratical sensitivity. The thermocouples voltages are acquired in differential mode, HI and LO floating, in order to reduce the common mode noise and the ground loop. In remote operations the HP34420A digital filters are not recommended; it requires more consecutive measures, while our program performs an acquisition only when requested. The signal noise is minimized setting a long integration time (20 NPLC); in addition, during the data processing, the average of the last 100 acquired values is made.

The thermocouples measures must be correlated to reference signals: the LN_2 and LHe levels, the pressure in the vacuum chamber and in the insulation vacuum and the i.b. temperature, read by a Carbon Glass Resistor (CGR). All these signals are acquired by the mux HP 3497A, 5 digit.

The heat power to the sample is provided by an Agilent E3646A programmable power supply, operated in constant-voltage mode with zero output impedance. The heater connection is made using remote sensing to correct the lead-load problem. The power supply is IEEE488 controlled and returns to the system voltage and current values.

The hardware components (the apparatus, the instrumentation rack and the PC) are connected to ground in an only point by a copper wire of 50 mm^2 of section.

2.2 Software

The software acquisition is developed in LabView 8.5. LabView has all the features and functionality of a traditional text based language, but with intuitive, graphical development and high level tools allow a fast development for measurements applications.

The basic building block of a LabView application is the Virtual Instrument (VI), which consists of a front panel and a block diagram.

Because the execution order in LabView is determined by the flow of data between nodes and not by sequential lines of text, multiple operations can be made in asynchronous mode. In this way, the program is interactive with the user and allows to modify or to recall the measure parameters when the application is running.

In Fig. 4 the flowchart of the program is shown.

When the application is started and the data filename is entered, the user can set the data acquisition and storage time rate, the default is 30 s for the reading and 60 s for the storage.

The Front Panel, Fig. 5, allows to the user to control the measure in progress. It has the double function of setting and visualization-control on the running measure.

The screen shows in real time: the time rate setting, the number of stored measures, the cryogenic levels and the vacuum values. The thermocouples values, in volt or in Kelvin, are plotted, the axis scale can be automatic or set by the user.

Two virtual switches on the monitor respectively recall in graphic way the whole measure in progress and one of the previous measures. The pc memory assigned to the real time graph can present only the last 6-7 hours of measurements, while a run lasts some days. The virtual switch "Full Measure" recalls all the data acquired: X axis shows the number of the stored measures, the first Y axis the thermocouples value and the secondary Y axis one of the measure parameters (cryogenic levels, vacuum, applied power). The graphical switch "Old Measure" recalls an old measure, which is stored in a proper database. This feature allows a comparison during the measure.

On the front panel the user can define the number of heating steps and the duration of every measure. The power steps number depend on the consumption of cryogenic fluid and on the time required to reach the thermal stability. A LN_2 run, 9000' of autonomy, allows to measure eight thermal conductivity values, the steady-state of every power step is reached after about twelve hours. The nitrogen refill is not possible without affecting the measure, as described later. A LHe run takes about 2300', with a refill during the measure. Also in LHe run it is possible obtain the steady-state for eight power steps, five hours for every power value.

After the power-on and the timer setting, the system of measure runs stand-alone. Only the vacuum chamber gate valve and the cryogenic fluid refill are manually controlled.

An additional routine developed with LabView Data Socket facility, allows to every pc connected on the LASA network to follow the measure.

3 MEASUREMENT METHOD AND PROCEDURE

The thermal conductivity is measured by the axial heat flux stationary method. The thermal conductivity is determined knowing the heat flowing per unit of area and the thermal gradient when the thermal equilibrium is reached. From the Fourier-Biot law:

$$\lambda\ (T) = -\ \frac{\dot{Q}}{S}\frac{dl}{dT}$$

approximating dl/dT with $L/\Delta T$ and considering S as a constant:

$$\lambda(\bar{T}) \cong \frac{\dot{Q}\,L}{S\Delta T}$$

Where L is the distance between two points along the sample, ΔT the corresponding difference of temperature, S the cross-sectional area and $\dot{Q}$ the heat flowing in the sample.

The Approximate Derivative Method (DAM) allows to determine the approximate value of the thermal conductivity at average of the two measured temperatures. In general measurement of λ is more precise as ΔT gets smaller. However if $\lambda(T)$ is a slowly varying function of temperature, the error is very small even if ΔT is few tens of degrees [4].

It is necessary to specify that if ΔT is too small the instrumentation error becomes predominant, as shown for LN_2 measurements later.

A run consists of cooling a sample to the reference temperature, LN_2 or LHe, then a heat flux is produced by a manganine wire heater.

The apparatus has been designed in order to make the parasitic losses negligible. The thermal equilibrium is reached when the thermocouples voltage stability is ± 100nV.

Sequence of the cryogenic operations with reference to the Fig. 1:

- Vacuum in Chamber by means of a turbomolecular pump. About 24 hours are necessary to reach 10^{-4} mbar.
- He gas into the Vacuum Chamber to 1 mbar, to avoid damp residual during the LN_2 reservoir cool-down.
- Vacuum in Cryostat, about 72 hours to reach 10^{-5} mbar.
- Cool-Down of the LN_2 reservoir and vacuum into Cryostat down to 10^{-6} mbar.
- Restore the Chamber vacuum to 10^{-4} mbar.
- Cryogenic fluid in the LN_2 / LHe Reservoir.

After this procedure the pressure value is $1.5 \div 2.5 \cdot 10^{-6}$ mbar, both in the Cryostat and in the Vacuum Chamber the vacuum remains acceptable for at least one week.

In order to allow the sample to reach the cryogenic temperature in a rapid and uniform way, He gas at ~ 5 mbar is put in the Chamber. Three hours later the vacuum chamber is restored to 10^{-6} mbar. The stability is obtained after 12 hours for LN_2 and 5 hours for LHe.

The average of the last 100 values of every thermocouple measurement at the cryogenic fluid temperature represents the zero of the measure.

The difference between calculated average and the Rosenbaum's values [5] (thermocouples emf normalized to 4.215 K or to 77.34 K) is the offset by which every thermocouple measurement must be corrected.

A power is selected and the measure can start. When the thermal equilibrium is reached, from the averaged measure of every TC the offset is subtracted and the net voltage is converted in temperature value using the Rosenbaum's data.

In the range 4÷100 K some functions are used in order to improve the precision of the conversion. For the LHe measurements, 4÷40 K, a LabView VI locates in the database, from the real TC voltage (average value measured minus the offset), the ten closest voltage values, 5 greater and 5 smaller, then the program relates them with the correspondent values in temperature. A polynomial function is obtained from the temperatures and the correspondent values of tension is calculated. For the LN_2 measurements a polynomial function is computed from the last 12 values (from 45.2 to 85.2 K) from Rosenbaum's database and normalized to 77.34 K.

The support system conductance (conductive heat losses) corresponding to the average temperature of the sample is calculated: the method is described in the paragraph 5.

The conductive losses are subtracted from the heater power measured (V·I) and the result is the net heat flux in the sample.

Finally, the thermal conductivity is calculated by Fourier-Biot formula, referred to the average temperature of the sample.

4 DEBUGGING OF THE APPARATUS MEASUREMENTS

4.1 Capacitive effect of the level probe during LN_2 refill in the thermal shield.

The nitrogen refill influences the TCs signals and some hours are needed to reach again the equilibrium.

The principle of measure of level nitrogen probe (Capacitance Liquid Nitrogen Level Probe - Magnex Model E5030) is the cause of this problem. The probe is constituted by two coaxial tubes insulated from each other, which form the electrodes of a capacitor. The liquid nitrogen is the dielectric. When the level of liquid varies, the dielectric changes and so the capacitance value.

An oscillator senses the capacity change and converts the frequency in a tension proportional to the LN_2 level.

The apparatus is not electrically insulated from the level probe and from its electronics. When LN_2 reservoir is refilled, two phenomena happen influencing the thermocouples measurements: a fast capacitive charge and a very slow discharge.

The problem has been solved realizing a new level meter, based on carbon resistor probe.

The probe is constituted by a G11 tube of Ø 7 mm and 1200 mm long, with 20 carbon 90 Ω resistors positioned at a distance of ~ 60 mm one from the other.

The resistors series is measured with a four-wire circuit using a 1 mA high stability current generator. This low current value does not affect the sensors with self-heating and the nitrogen vapour generation is avoided.

The probe has been calibrated with respect to the capacitive probe. The function obtained is inserted in a LabView VI to the voltage/level conversion.

In Fig. 6 the capacitive effect of the LN_2 refill on the measurements is shown.

The graph time scale shows 130 hours; the starting condition is the thermal equilibrium, with thermocouples voltage in a steady-state situation. When the LN_2 refill begins, marked in figure, a signal overlaps with the TCs trend. The voltages increase by 1-1.5%, with reference to the TC4, TC6 and TC7, that have a larger absolute value. Two refills have been made in this run. Every thermocouple, when the refill starts, has a different voltage value, but the relative growth is almost identical.

The phenomenon is characterized by two time constants: the first one, about 2 hours, is due to refill; the second, after refill, shows that the TCs voltage approaches the initial value without achieving it, also after a very long time.

4.2 Pressure value influence on Zero procedure.

Helium gas is let in the Vacuum Chamber so that the sample reaches rapidly and uniformly the thermal equilibrium. After three hours a vacuum of 10^{-6} mbar is restored. The TCs voltage value measured during this procedure is practically constant with a gas pressure from 0.1 to 10 mbar, as shown in Fig. 7. We work at 5 mbar since a too large pressure would increase heat flux to the sample chamber wall.

In the Fig. 8a and 8b the gas and vacuum zero conditions are compared for every thermocouple referred to its position, considering TC1, on cold heat sink, to 0 mm. [(1)]

The TCs voltage values in gas-vacuum LN_2 condition are contained in a very narrow range, ±1μV, Fig. 8a.

At LHe temperature the TCs voltage difference between gas and vacuum condition is more evident and the vacuum repeatability is better, Fig. 8b.

The TC5 both at LN_2 and at LHe temperature does not follow the other sensors behaviour.

4.3 Thermocouples construction

The thermocouples are constituted by two wires, one in Au-Fe (0.07% at.w.) and the

[(1)] Fig. 14 shows the sketch of an Nb3Sn sample built with ceramic tape + binder, provided by the Fermilab. The image is sectioned and exploded to show the thermocouples position on both sides of the sample.

other in Cromel P. Every wire, Ø 0.127 mm, is insulated by thin layer of teflon which must be removed before welding. A twisting is made for conferring them a certain consistence in the welding area. Thermocouple Welder mod. 125 of the Netzsch is used.

The welding of the thermocouple is done by placing the wires into the wire holder, inserting the holder into the weld cavity and creating an atmosphere of inert gas.
Some shrewdness is required to solder the wires on the i.b.. The bare Cromel wire oxidizes instantly, it is therefore necessary the use of a decapant flux (Fontargen liquid F600). During the soldering the Au-Fe wire melts inside the soldering alloy (Sn 60%, Pb 40%). To avoid this, the wire is quickly dipped in the molten. In this way the soldering is made at a lower temperature.

A new alloy (In 80%, Ag 5% and Pb 15%), with a lower melting point is under test.

4.4 TC1 electric isolation

The thermocouple TC1 is inserted in the heat sink; this is a copper block electrically connected to measure apparatus and therefore not ground floating, therefore an undesirable connection affects the TC1 emf. For this reason a galvanic isolation of thermocouple is provided by 70 μm Kapton tape.

In Fig. 9 the improvement of the TC1 acquired signal is shown. The comparison is made with TC2 sensor, galvanically insulated.

5 HEAT LOSSES

In Fig. 2 the measurement system is shown. A stainless steel chamber encloses it, a turbomolecular pump maintains the internal pressure at about 10^{-6} mbar and the vacuum seal is guaranteed by an indium o-ring.

In order to evaluate the conductivity and the net power flux through the sample, the heat losses due to conduction, convection and radiation must be estimated.

Broggi and Rossi [1] have devised a mathematical model for every type of thermal loss. The convective losses can be reduced to a negligible value by operating at 10^{-5} mbar; the radiation losses are 10^{2} times lower than the power flux, if the difference of temperature between the sample and the external wall of vacuum chamber (temperature of the cryogenic fluid) is lower than 20-30 K. Finally, the conduction losses are evaluated computing the heat flux through the sample supporting system.

The indications of report [1] are considered to assess the convection and radiation losses, while for the conduction ones a series of blank measurement were made.

In this specific case eight thermocouples are positioned on the sample pressing system; which is regulated by four stainless steel rods as if the sample were present. Two TC are on hot heat source, two on cold heat sink, one on G11 pressing plate, one on middle of a rod and two on isothermal block.

The power flows into a sequence of materials thermically connected in series, from the heater to the pressing plate and through the stainless steel rods to the cold heat sink. This mechanism is the parasitic conductance of the system.

In Fig. 10 the values of conductance measured here are compared to the calculated and measured ones by [1].

The function obtained by the measured points allows to calculate the losses, Q_{loss}, for every intermediate temperature value of the sample.

6 TORLON MEASUREMENTS

The Torlon [6] is an amorphous organic polymer which exhibits interesting mechanical properties (low coefficient of linear thermal expansion, high creep resistance, and excellent compressive strength) and a good chemical resistance throughout a wide temperature range; in particular it retains its high strength at cryogenic temperatures.

Barucci et al. have measured the thermal conductivity of Torlon 4203 PAI Polyamide-imide (Solvay Advance Polymers, L.L.C.) in the range of temperature 4.2÷300 K [7].

Fig. 11 shows our cylindrical sample in Torlon and the set in thermocouples. We have measured the conductivity around four cryogenic temperatures: 6.1 K, 10.7 K, 77.6 K and 78.2 K.

In Fig.12 our data are compared with those of Barucci [(2)]. The sample supporting system and the temperature sensors are different but this is not a priori an explanation. Our number of measured points is smaller, but there is no doubt that our values of the conductivity are higher. We fear that the measured Torlon is not exactly the same.

The conductivity has been measured using two thermocouples positioned at different distances from each other and on different sides of the cylinder. The resulting values are practically the same since the sample is constituted by homogeneous material.

The spread of the values near LN_2 temperature is due to a ΔT too low between the hot source and sink: in this case the instrumentation error is dominant.

7 Nb3Sn OLD SAMPLES

Early in 2007 a series of measures was made with an Nb3Sn sample with ceramic insulation, already characterized in 2002 [8].

In Fig. 13 the results of our measurement and those from [8] are compared.

In our measures only two temperature values are considered: LHe and LN_2.

The number of measured points is different, but the agreement seems reasonable.

8 Nb3Sn FERMILAB SAMPLES

In 2007 the thermal conductivity of some Nb3Sn samples with ceramic tape and binder, provided by Fermilab, has been measured. These samples have been manufactured from the same cable.

---

(2) Barucci et al. claim the effect of thermal resistance between the sample and the copper blocks is considered equal to 2% of λ, two carbon thermometers are positioned on the heat sinks.

In Fig. 14 a sketch of the sample is shown, the image is exploded to show the position of the TCs on both sample sides.

Two samples, denominated A and B, with thermocouples holes, were provided by the Batavia laboratory. A third sample, named C, was cut in our Laboratory but not with same results, because an appropriate mechanical equipment is necessary and the LASA does not have it.

A local resin detachment and the resulting uncovered superconductor wires, are present on the upper side of sample A. Our sample C has a fracture of 12 mm near the TC7 hole.

In Fig. 15 the thermal conductivity of the three samples is compared.

The conductivity difference of the samples A and C is ± 10% from LHe to 110 K compared to that measured for the sample B; B points can be considered intermediate values.

In Fig. 15b the thermal conductance determined from the temperature value of TC1 on the cold heat sink and of TC8 on hot heat source is shown. This value also includes the contact thermal resistance between the heat sinks and the sample. These results remark the difficulty to get equal measure conditions despite the care devoted to sample assembly.

The sample B has been measured several times; the measure runs are named in time sequence B, B1, B2, B3 and B4.

The LN_2 measures are presented in Fig. 16a, 16b and 16c; those at LHe are shown in Fig. 17a, 17b and 17c.

The graphs with suffix **a** and **b** show the conductivity along the sample, the graphs **c** present the thermal conductance between TC1 and TC8, including the thermal contact resistance at the interfaces.

At LN_2, if the heating power is less than 5 mW, the temperature difference between two close sensors is so small that the conductivity evaluation is distorted and the error inducted becomes dominant. We believe that ΔT must be at least 1 K.

The conductivity spread at LN_2 is 30 mW/m·K (5% of the average value), in Fig. 16a and 16b; and 30 mW/m·K (11% of the average value) at LHe, in Fig. 17b.

The conductance values to LN_2 and LHe, figures 16c and 17c, demonstrate the repeatibility of the measurements, between different thermal runs (cool down), each involving the sample assembly and disassembly.

The TC2 and TC3, TC6 and TC7 are positioned in the same superconductor layer, as shown by Fig. 14. The TC2 and TC6 are on the vertical axis, the TC3 and TC7 at 6 mm from the sample edge. Theoretically the corresponding couples of TCs should read the same temperature, but significative differences are noticed by the measured values. For different samples (A, B, C) this could be justified by a different mechanical dimension, but this is not justified for the same sample (B) measured in different times.

Clearly the absolute temperature values do not change too much, but a small temperature difference (ΔT) affects the conductivity heavily.

This discrepancy among the results could be due to the thermocouples on the same layer in different position, which are not galvanically isolated from each other. At room temperature between the TC6 and TC7 position we have 1.3 Ω and between TC2 and TC3 1.7 Ω.

The non-homogeneous physical structure of the sample (alternate layers of superconductor and insulator) can be another reason, leading to larger differences between samples.

It would be opportune to consider as sample conductivity the average of those calculated with two or more TCs pairs.

A large number of measures, mainly with sample B, has allowed to test the software, to set up the apparatus and to verify the measure repeatability.

9 ERROR BUDGET

The different error sources of our system are analyzed hereafter.

9.1 Error due to isothermal block.

The measure principle is based on a heat flux through the sample from the hot to cold heat sink. The thermocouples leads are connected to a cold reference junction (isothermal block), that should be at the cryogenic fluid temperature. Nonetheless, by means of a CGR fixed on this support we have noticed a change of temperature, increasing with the heating power.

At LN_2 temperature the rise in temperature of the i.b. is 2% with 500 mW. The software compensation of this variation reduces the thermal conductivity of 0.5% on the whole range of measurements at LN_2 temperature, as shown in Fig.18a with reference to the sample C.

At LHe the i.b. temperature increase is limited to 2% up to 100 mW, but with 200 mW the rise is 34.6%. The compensation reduces λ of 0.35% to 20 K and of 2.8% to 30 K, see Fig 18b.

A VI for automatic correction will be developed for the next measurements and inserted in data analysis program.

100 mW is the maximum heating power for measures at LHe temperature.

9.2 Heat losses

To obtain the thermal conductivity of the sample only the conduction losses, evaluated from blank measurement, have been considered. We have also estimated the convection and radiation losses using the mathematical models developed by Broggi and Rossi [1].

If the pressure in the Vacuum Chamber is of the order of 10^{-6} mbar, with a sample average temperature of 100 K and 500 mW of power flux, the convection losses are 0.3 mW, or the 0.06%. At LHe with T_{avg} of 30 K and 200 mW, convenction losses amount to 0.2 mW, or the 0.1%. These losses are negligible.

The radiation losses are slightly larger: but also at the maximum sample temperature they are limited to 0.5% of the power supplied by the heater.

Another error source is the accuracy of the Agilent E3646A power supply, which provides the heating power. It is 0.5% or less in a four-wire configuration.

9.3 Dimensional error.

The error in form factor measurement, made with a digital calliper, has been estimated as 0.5% for L, and as 1% for the cross section, 0.5% for each linear measure.

This error is caused by the sample surface not perfectly flat (sample with ceramic tape and binder).

9.4 Error on the measure of temperature.

The error due to the thermocouple emf measurements can be considered equal to voltage sensitivity, including all the system contribution, 100 nV. Considering the TC average conversion rates from 4.22 to 85 K equal to 16 μV/K, the error is ~ 6 mK. This means that the error is 0.15% at LHe, while at LN_2 it is equal to 0.1%.

The accuracy of the Voltage-Temperature conversion is ±1.0% according [5], must be added to this error.

Finally, with reference to $\lambda(\overline{T}) \cong \frac{\dot{Q}L}{S\Delta T}$

the addition in quadrature of the errors in the λ gives:

$$\left(\frac{\Delta\lambda}{\lambda}\right)^2 = \left(\frac{\Delta Qeff}{Qeff}\right)^2 + \left(\frac{\Delta ff}{ff}\right)^2 + \left(\frac{\Delta(\Delta T)}{\Delta T}\right)^2$$

$$\frac{\Delta\lambda}{\lambda}\% = \sqrt{(0.5+0.5)^2\% + (0.5+1)^2\% + (0.15+1)^2\%} = 2.4\%$$

This error must be added to another 0.5% caused by the heating of the TCs cold reference junction (isothermal block).

10 CONCLUSIONS & FUTURE ACTIONS

We have upgraded the existing apparatus for thermal conductivity measurements with a new acquisition electronics and a new software. The performances and the limits of the instrumentations have been assessed. Some improvements will optimize the performance and the efficiency of the system.

The thermocouple construction and insertion into the sample is difficult and it is practically impossible to repeat the previous situation, both in the TC size that in their positioning. They are inserted in the holes in the sample and sealed with Cryo-Con®, and the pressure changes can affect their position.

The welding of the cold junction is not easy; in particular the Au-Fe wire quickly dissolves during welding, this could be solved by means of a new alloy.

The LakeShore, the wires supplier, considers the maximum achievable accuracy to be about 1%, with TCs realized by means of special techniques not better defined.

The realization of the TC holes, 1 mm in diameter, in the superconductor layers is difficult and inaccurate; a boring mask would be necessary. The non-homogeneous physical structure of the sample (alternate layers of superconductor and insulator) makes the drilling very difficult. The vibration of the jobber drill can crack the insulator, as we have experienced.

A future run of measure will be dedicated to quantify the effect of the lackness of electrical insulation between thermocouples.

Some software improvements are foreseen.

- A LabView VI to automatically compensate the temperature variation of the isothermal block.
- Knowing the time necessary to reach the temperature stability of the TCs is possible to realize a VI to evaluate the thermal conductivity for every temperature of the sample. On the last hundred values the average is made and the offset removed. The voltage–temperature conversion using the stored database allows calculating the λ for every couple of TC. The most meaningful data are then saved on an Excel sheet.

11 FIGURES AND TABLE LIST

12 ACKNOWLEDGMENTS

The authors are grateful to dr. Francesco Broggi, among the first ones working with the LASA thermal conductimeter apparatus, for his precious suggestions and to have furnished the calculated and measured data related to the thermal losses of the system.

13 REFERENCES

(1) F. Broggi, L. Rossi, Test of an apparatus for thermal conductivity measurements of superconducting coil blocks and materials at cryogenic temperatures, in: The Review of scientific Instruments, **67**, n. 9, (September 1996).

(2) F. Menotti, Misure ed analisi della conducibilità termica in superconduttori e materiali composite a basse temperature, in: Tesi di laurea, (UNIMI, AA 1993-94).

(3) Pratical Temperature Measurements, Application Note 290, , Agilent Technologies, USA, (© 2000).

(4) J. G. Hust , R. B. Steward, International Journal of Thermophysic, **3**, n.1, 66-77.

(5) R. L. Rosenbaum, Some Properties of Gold Iron Thermocouple Wire, in: The Review of Scientific Instruments, **39**, n. 6, (June 1968).

(6) Solvay Advanced Polymers, Poliammide-immide TORLON® Guida alla progettazione, (©2003).

(7) M. Barucci, E. Olivieri, E. Pasca, L. Risegari, G. Ventura, Thermal conductivity of Torlon between 4.2 and 300 K, in: Cryogenics, **45**, 295-299, (2005).

(8) L. Imbasciati et alt., Thermo-Mechanical Characterization of Insulated and Epoxy-Impregnated Nb3Sn Composites, in: IEEE Transactions on Applied Superconductivity, **13**, n. 2, (June 2003).

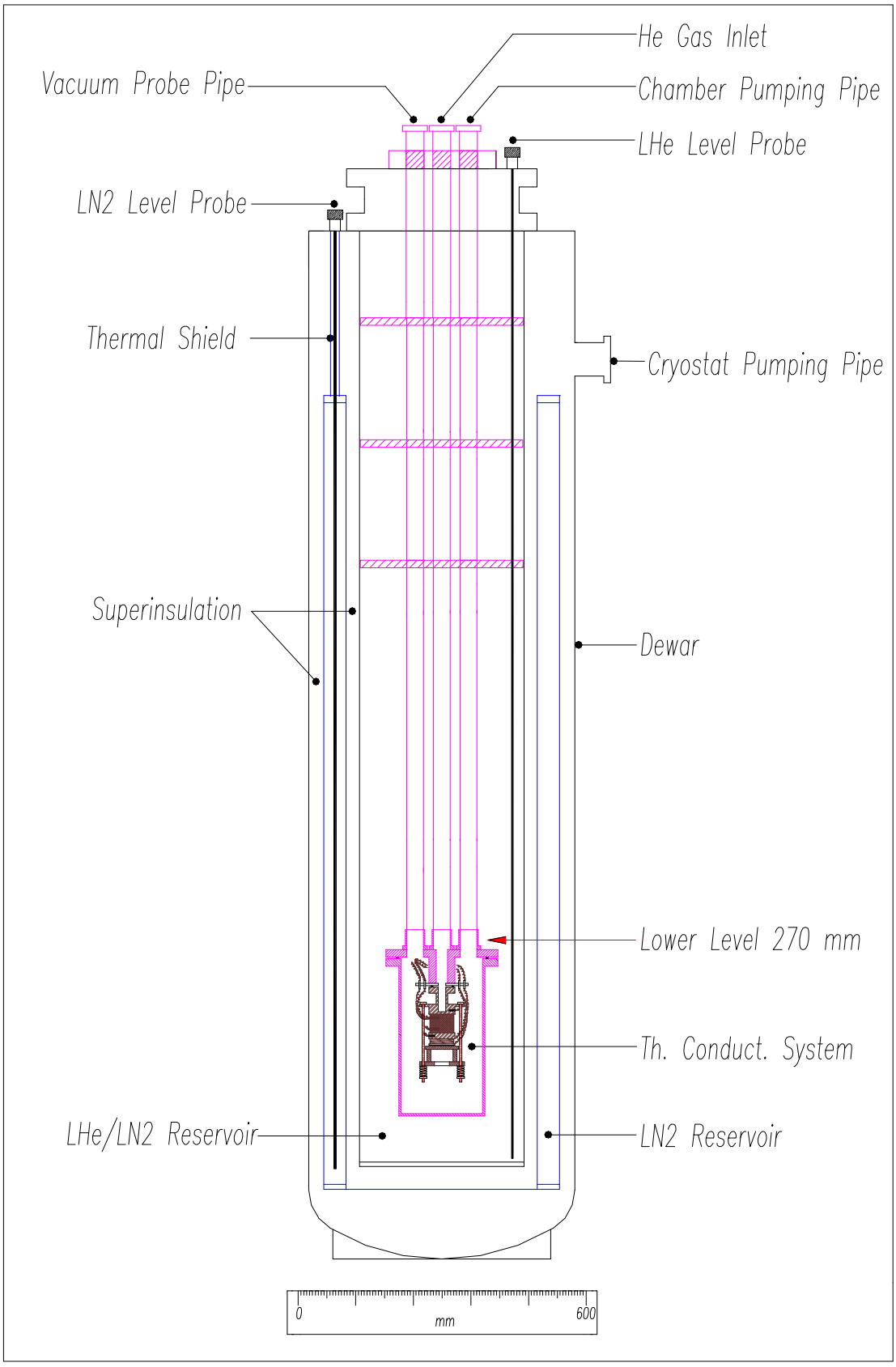

FIG. 1: Sketch of the Thermal Conductimeter Apparatus

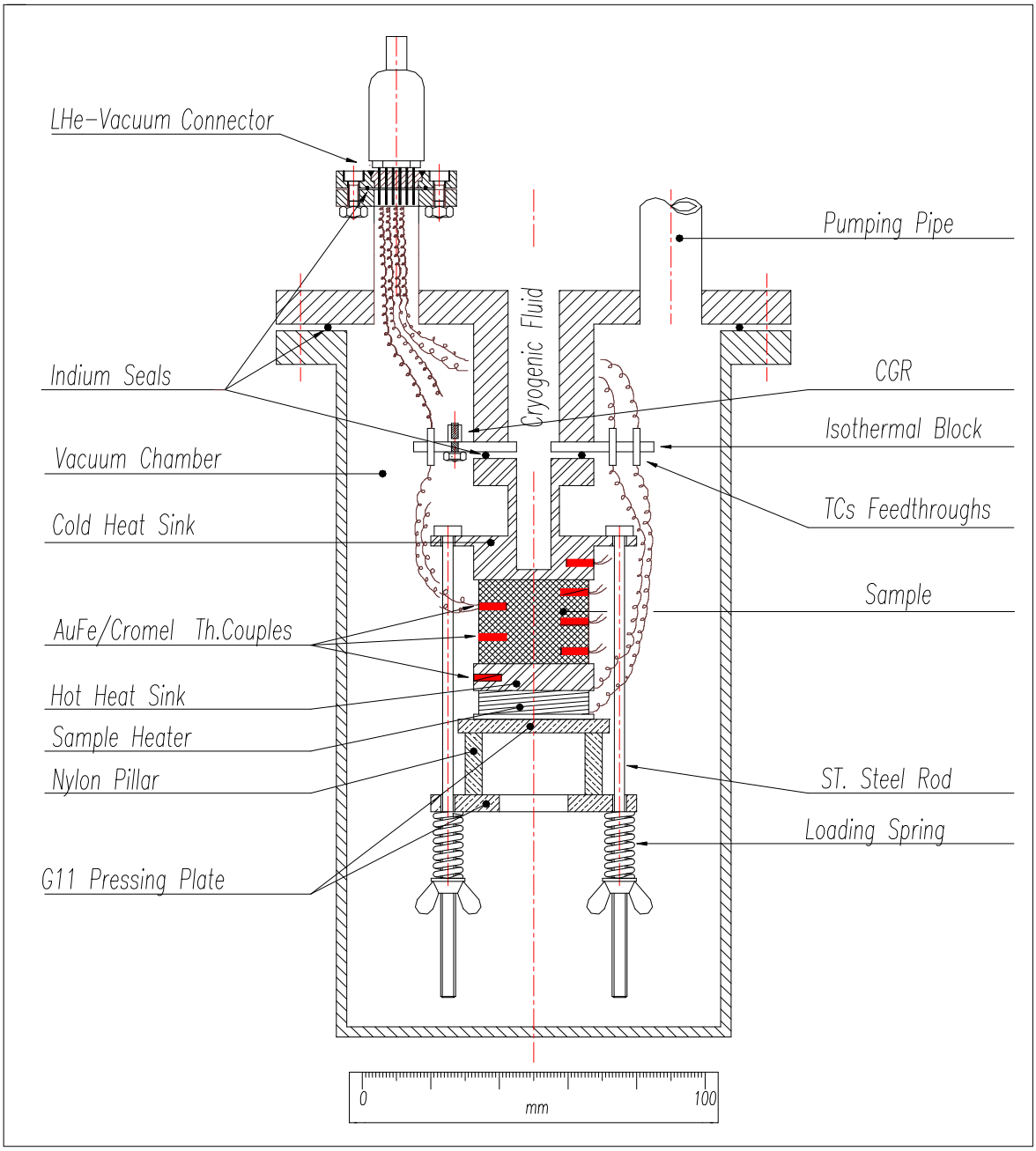

FIG. 2: Sketch of the Thermal Conductimeter System

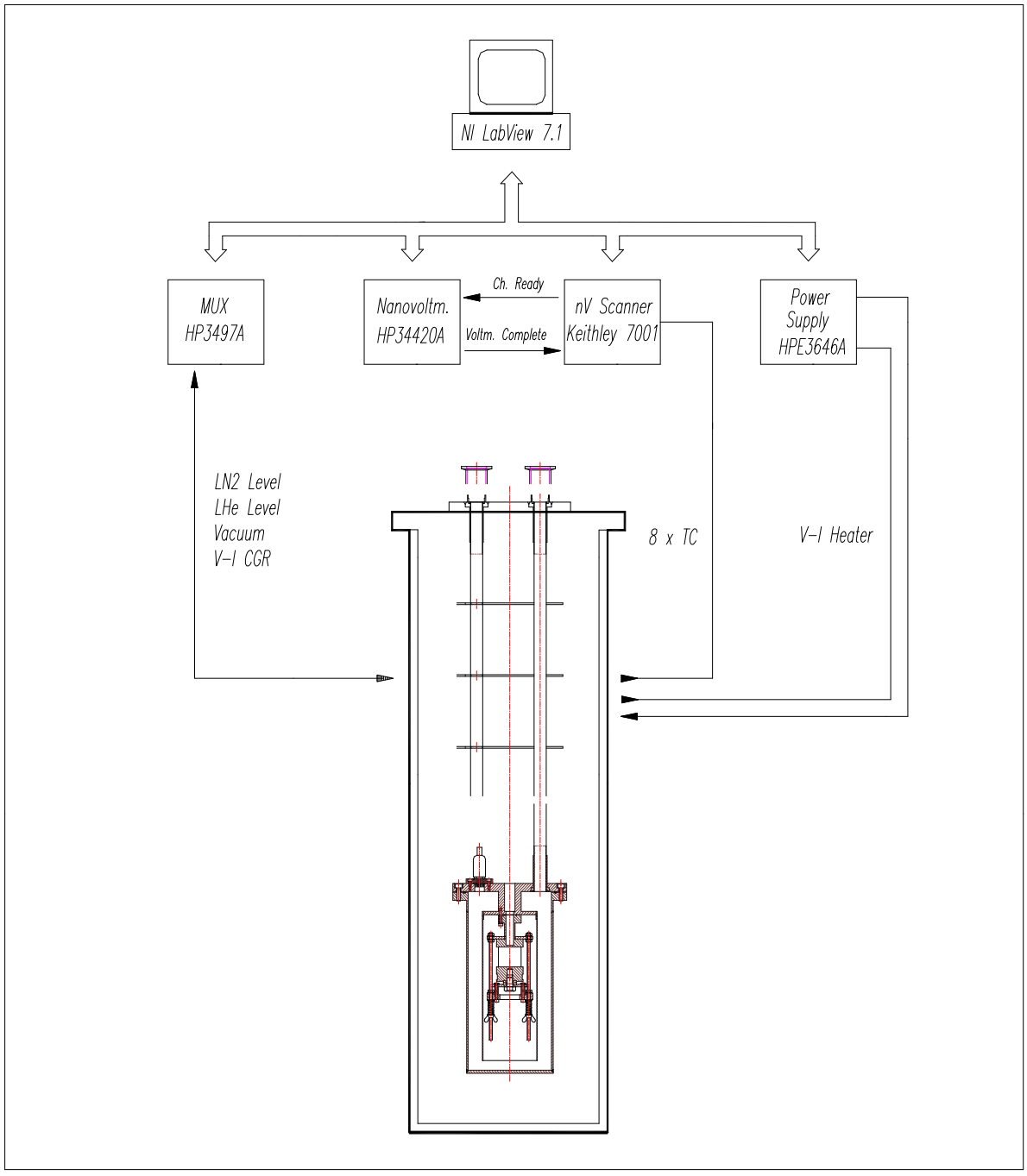

FIG. 3: Acquisition System

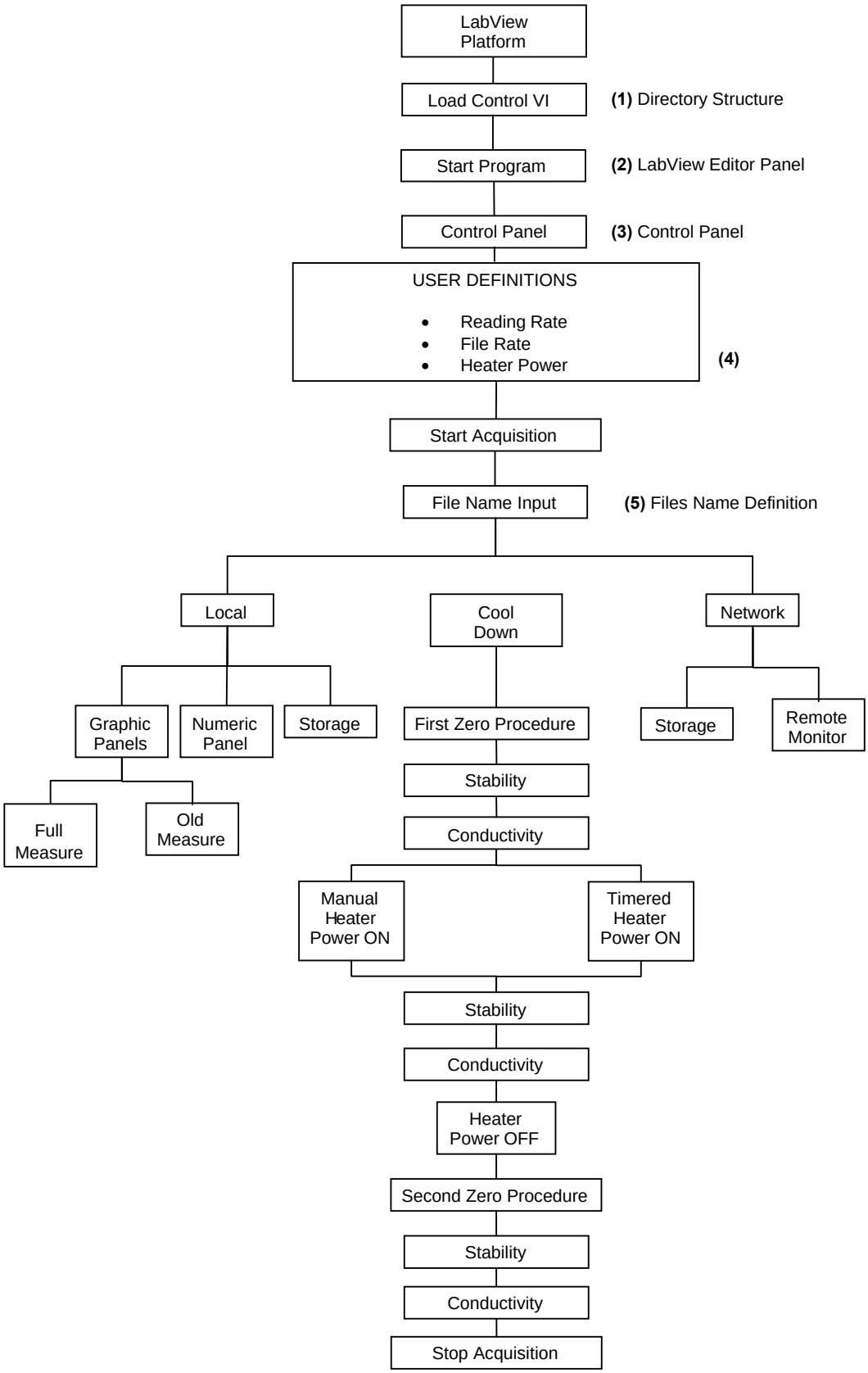

FIG. 4: Program Flowchart

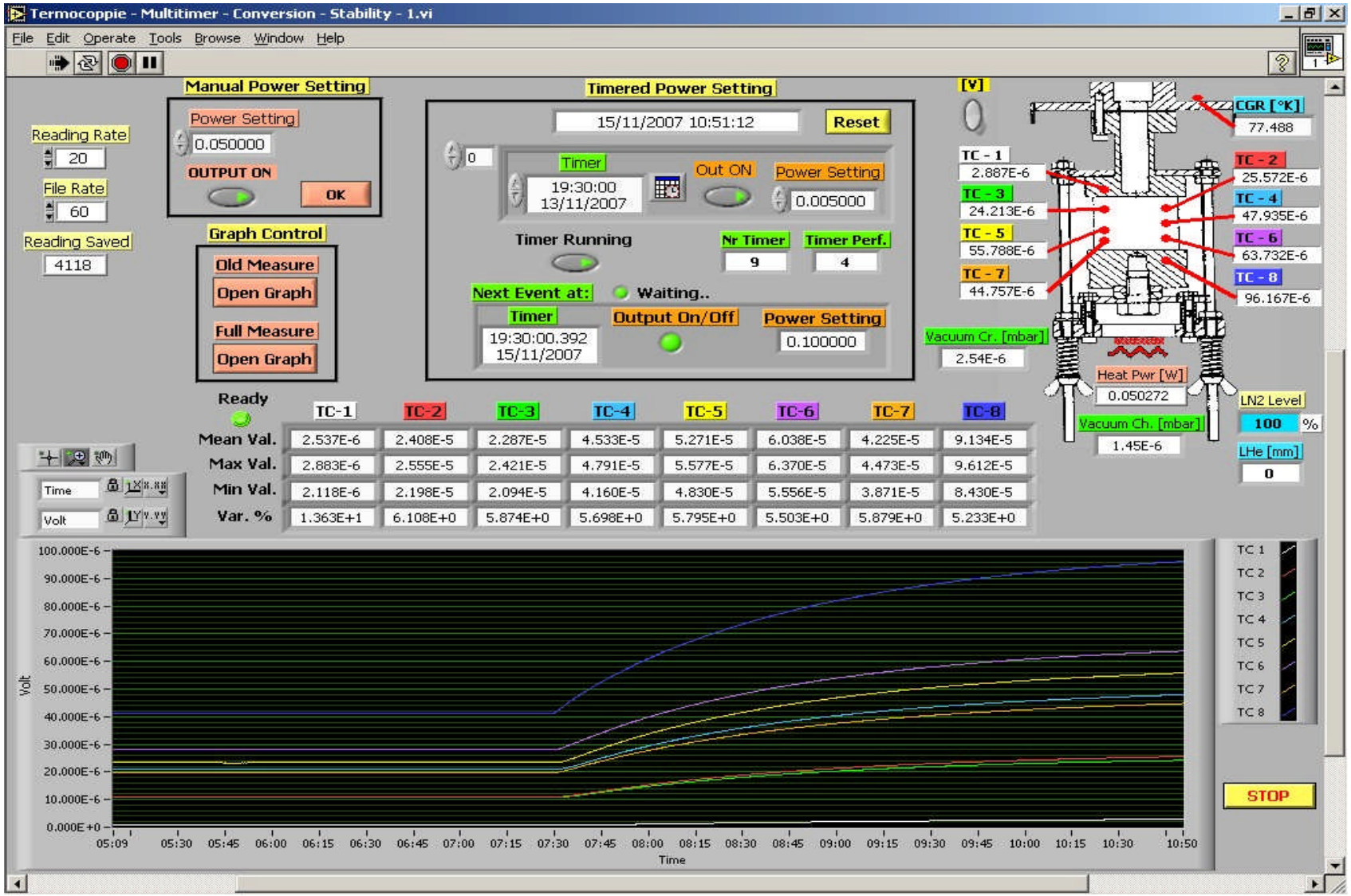

FIG. 5: LabView Front Panel

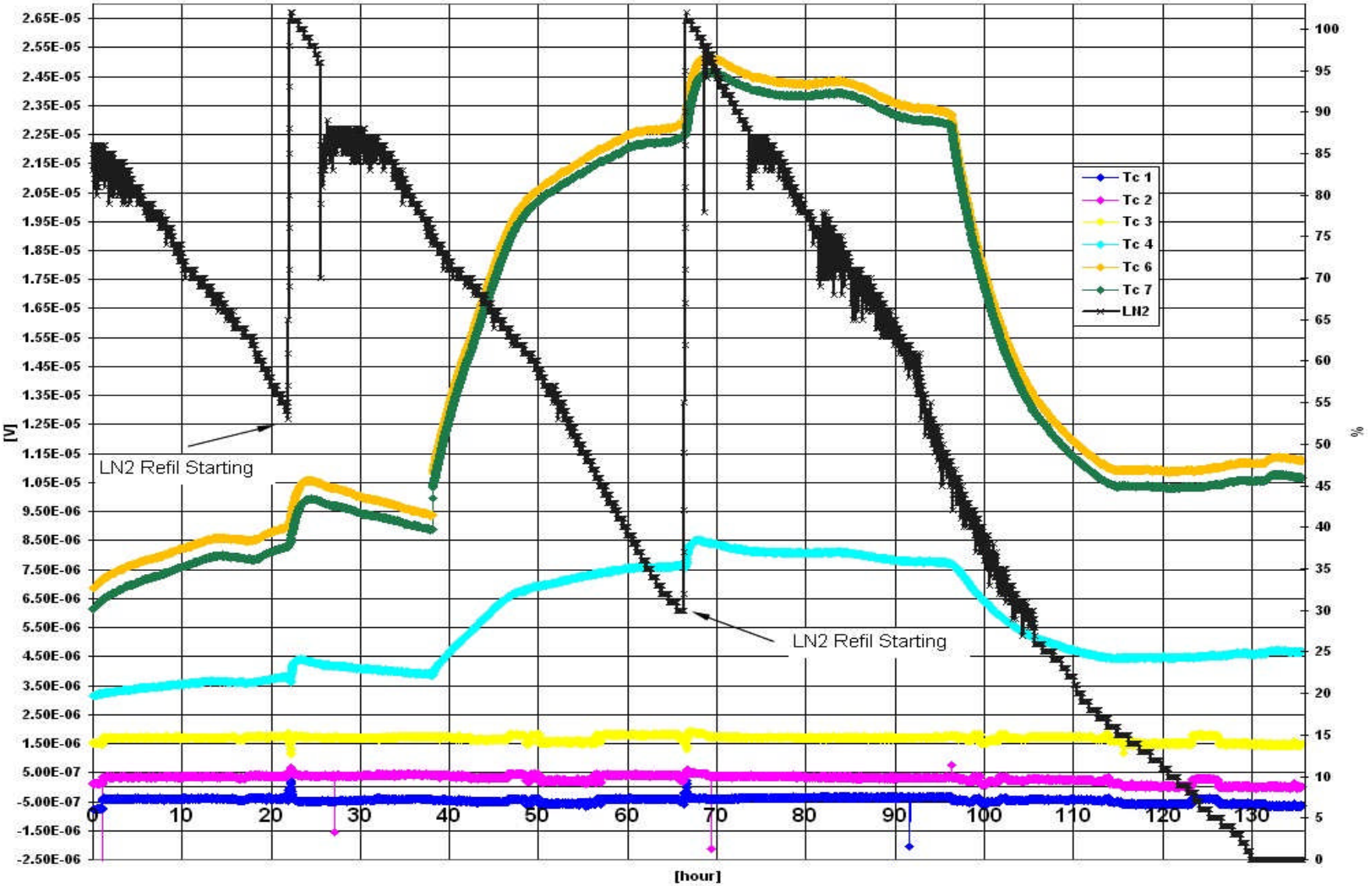

FIG. 6: Capacitive Effect of LN_2 Probe

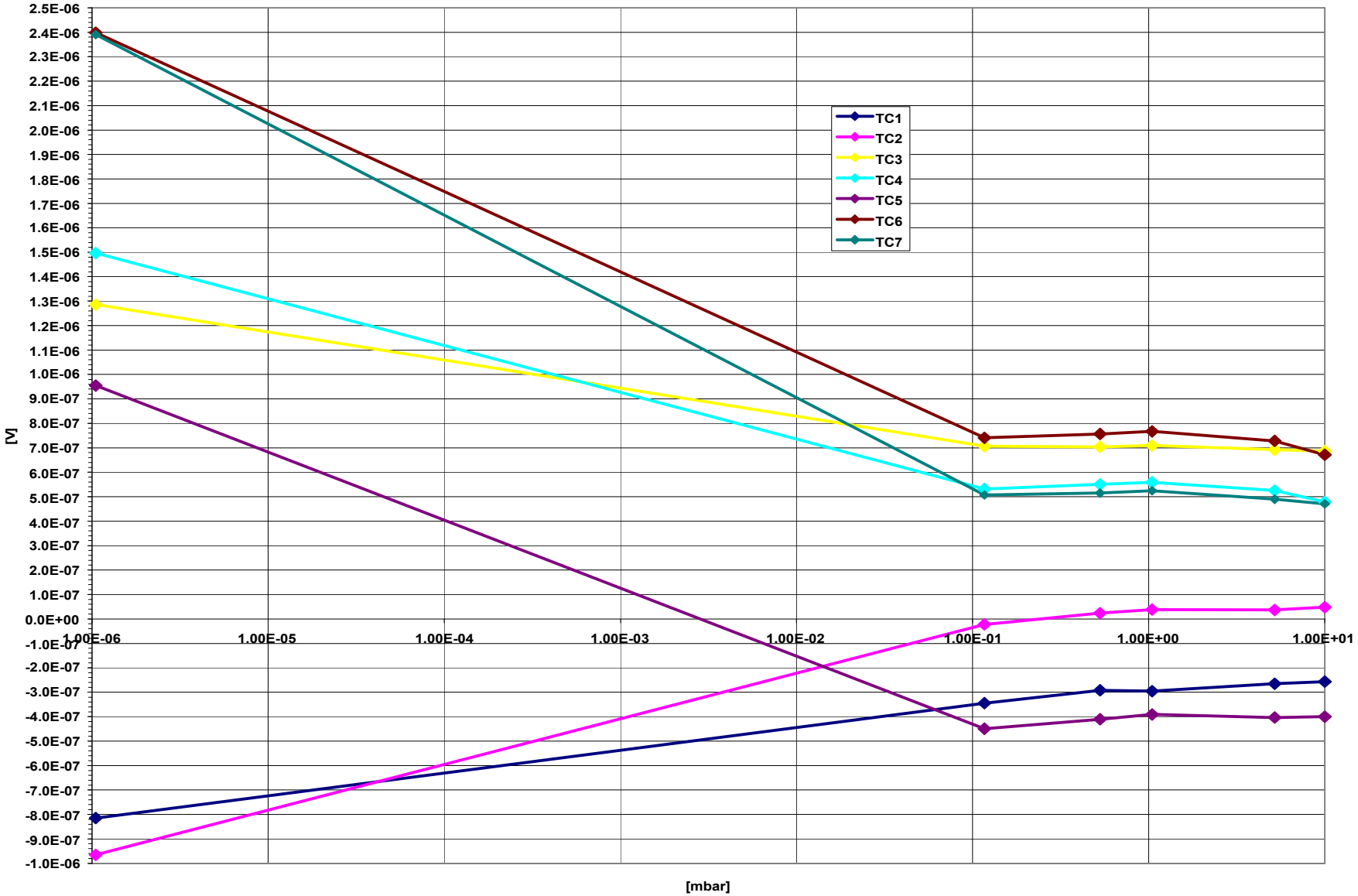

FIG. 7: Thermal Zero vs. He gas Pressure

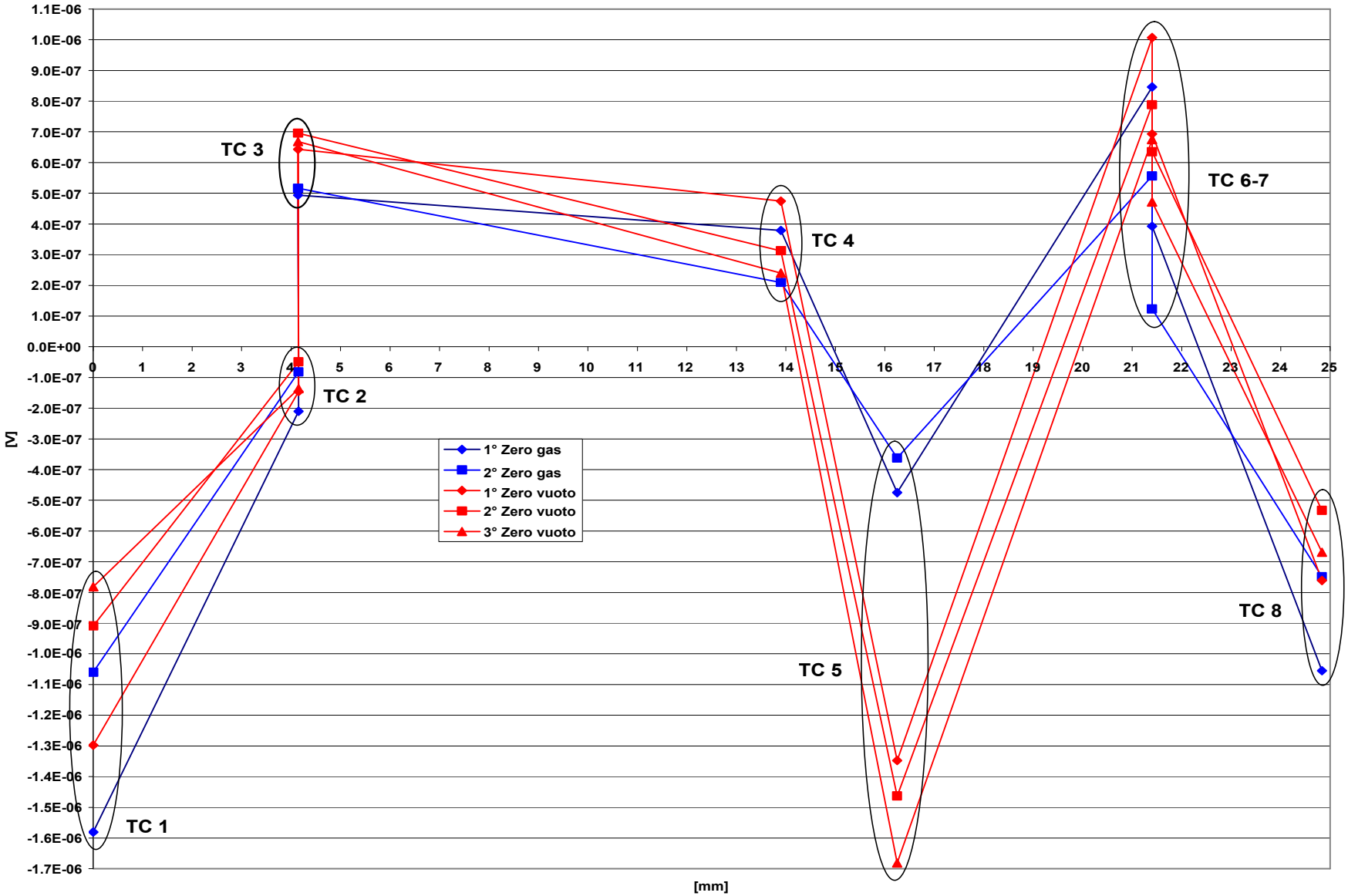

FIG. 8a: LN_2 Thermal Zero vs. TCs Position

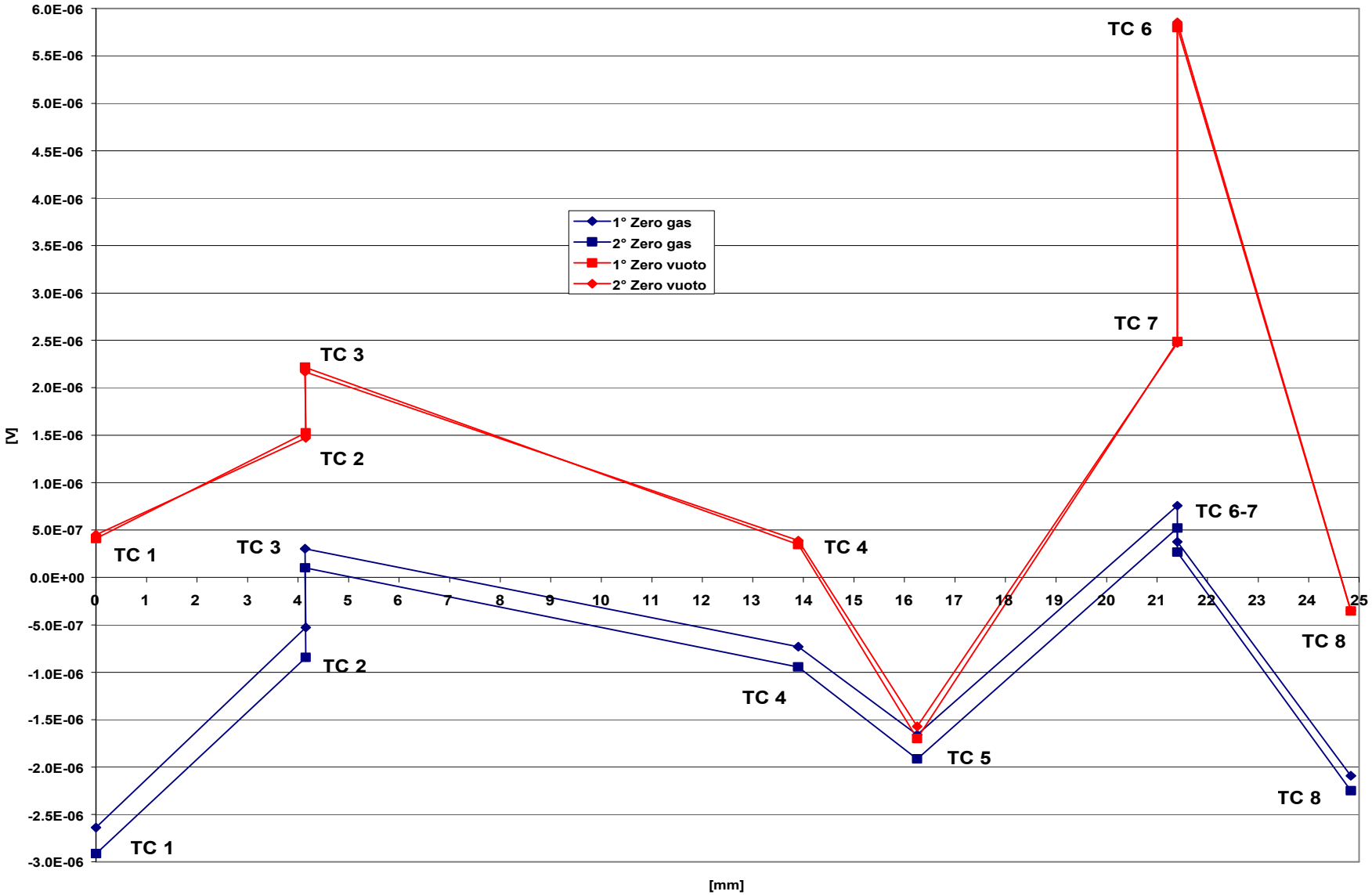

FIG. 8b: LHe Thermal Zero vs. TCs Position

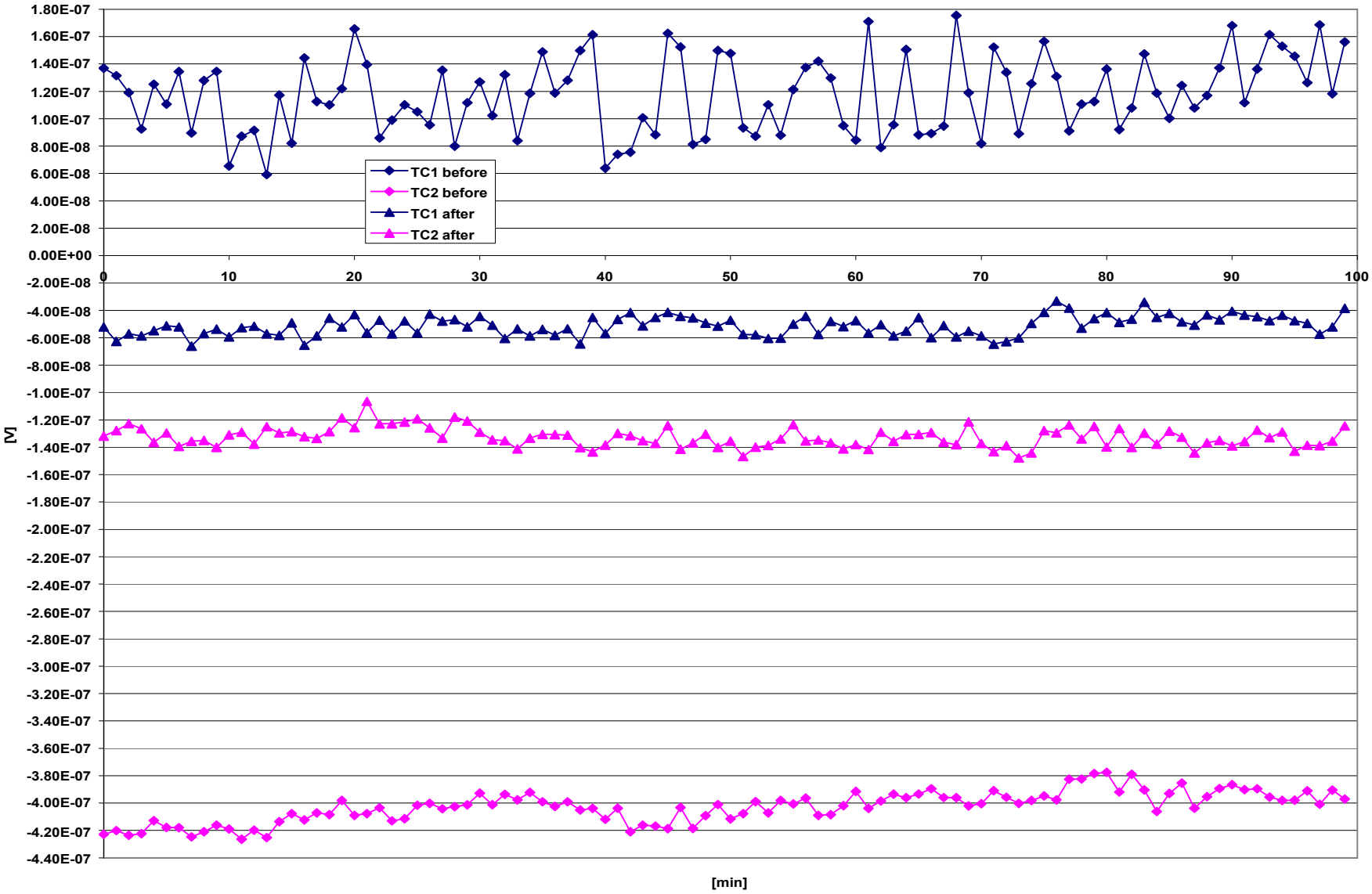

FIG. 9: TC1 Signal before and after Electric Insulation

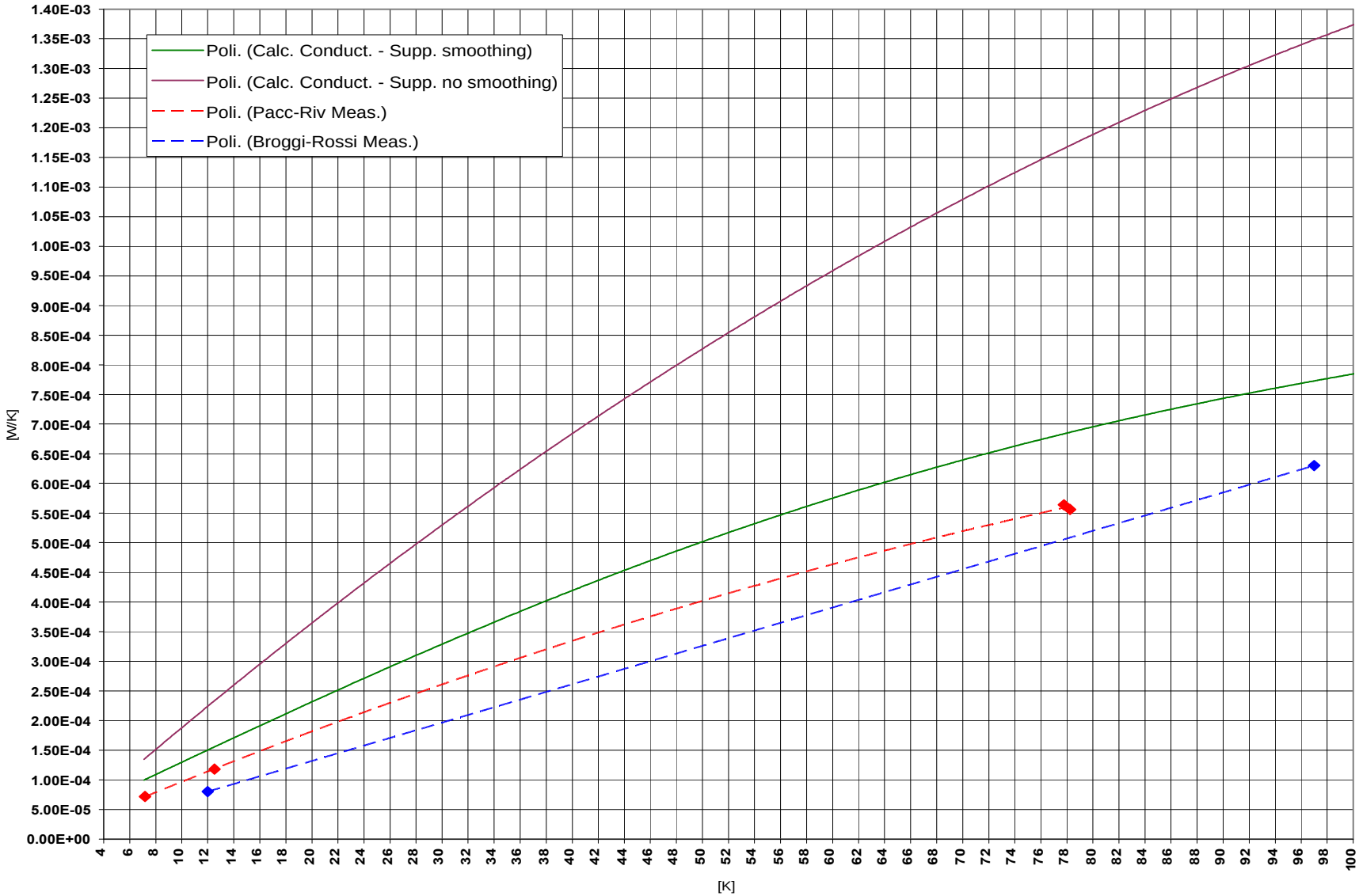

FIG. 10: Thermal Conductance of the Supporting System

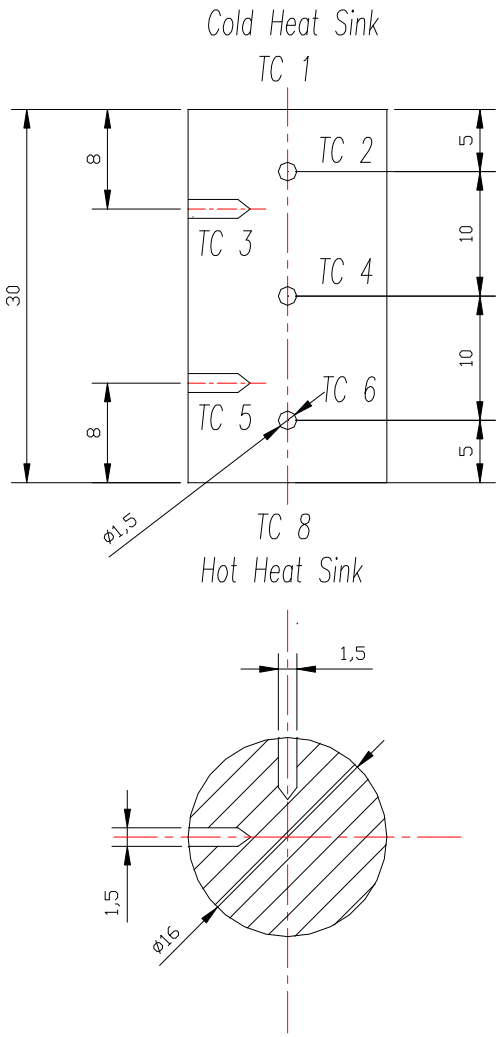

FIG. 11: Torlon Sample and TCs

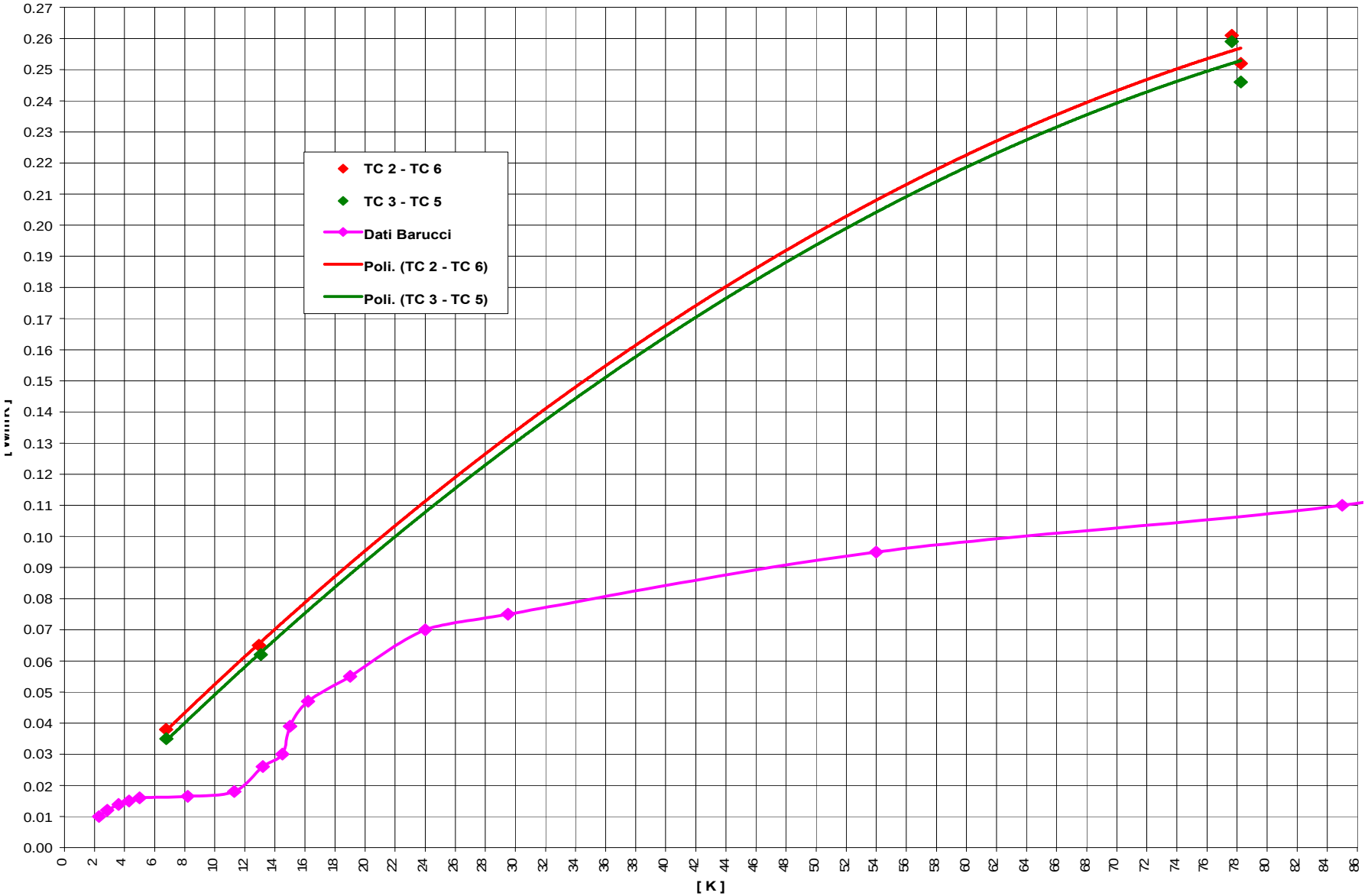

FIG. 12: Torlon Th. Conductivity

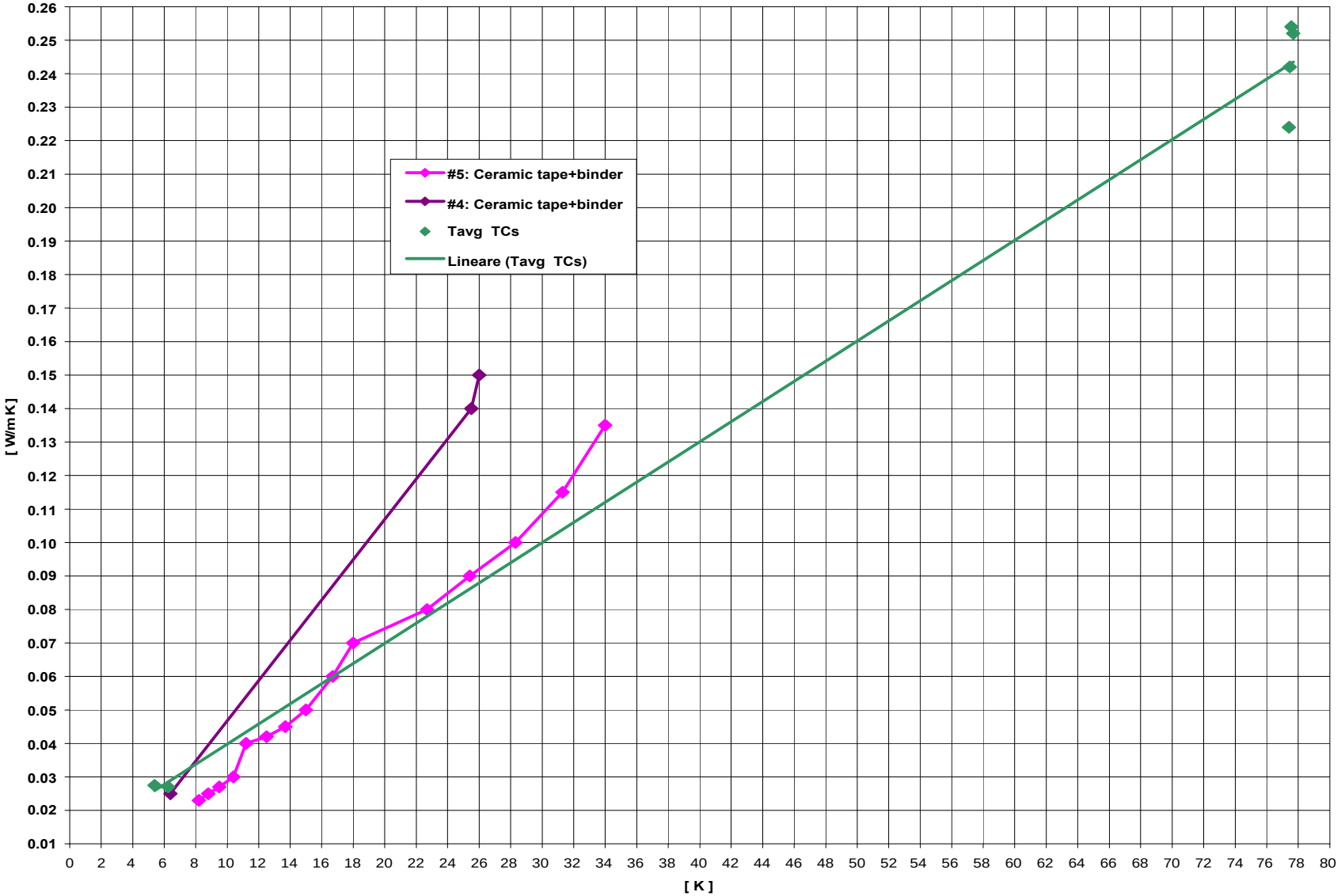

FIG. 13: Nb3Sn Old Sample Th. Conductivity

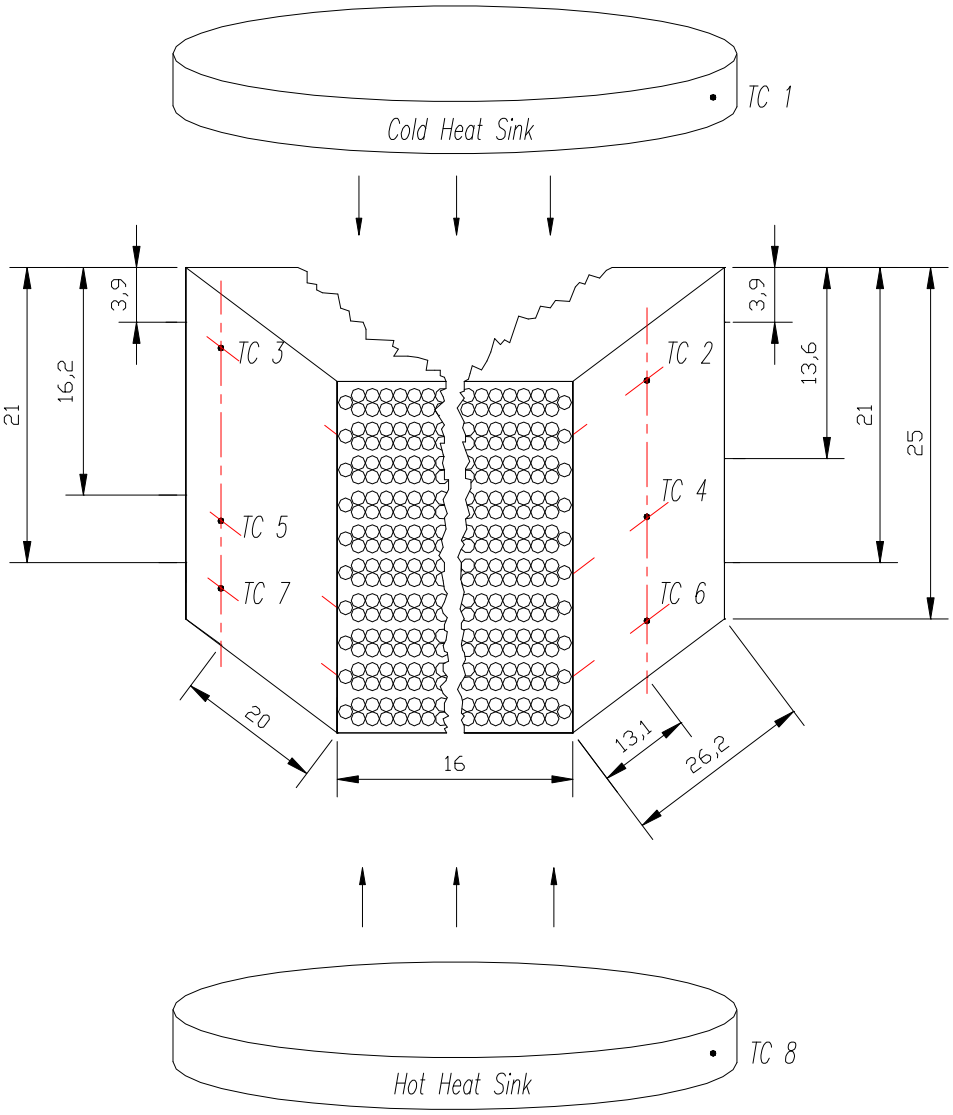

FIG. 14: B Sample and TCs

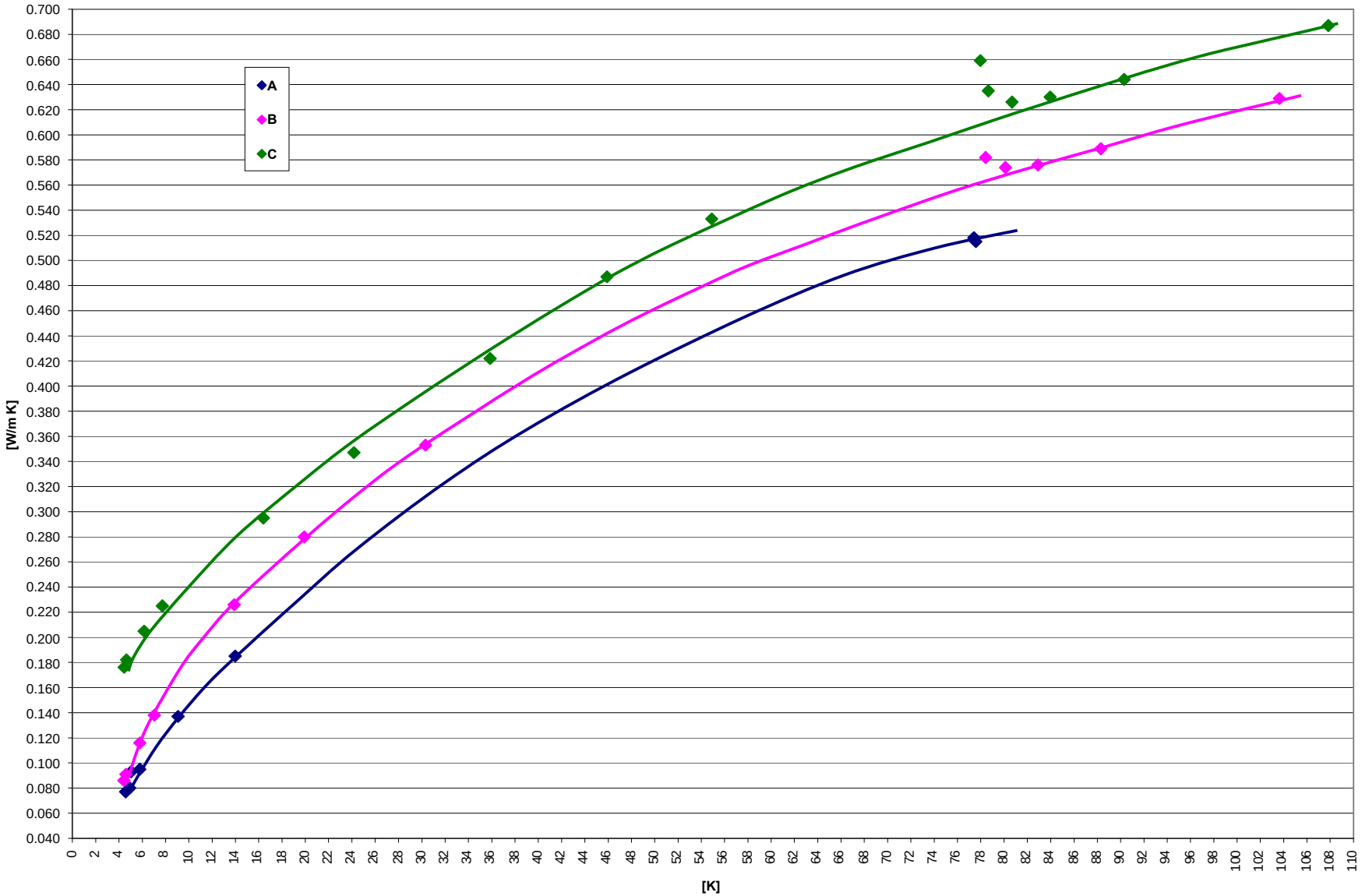

FIG. 15a: A, B, C Sample Th. Conductivity between TC2 – TC6

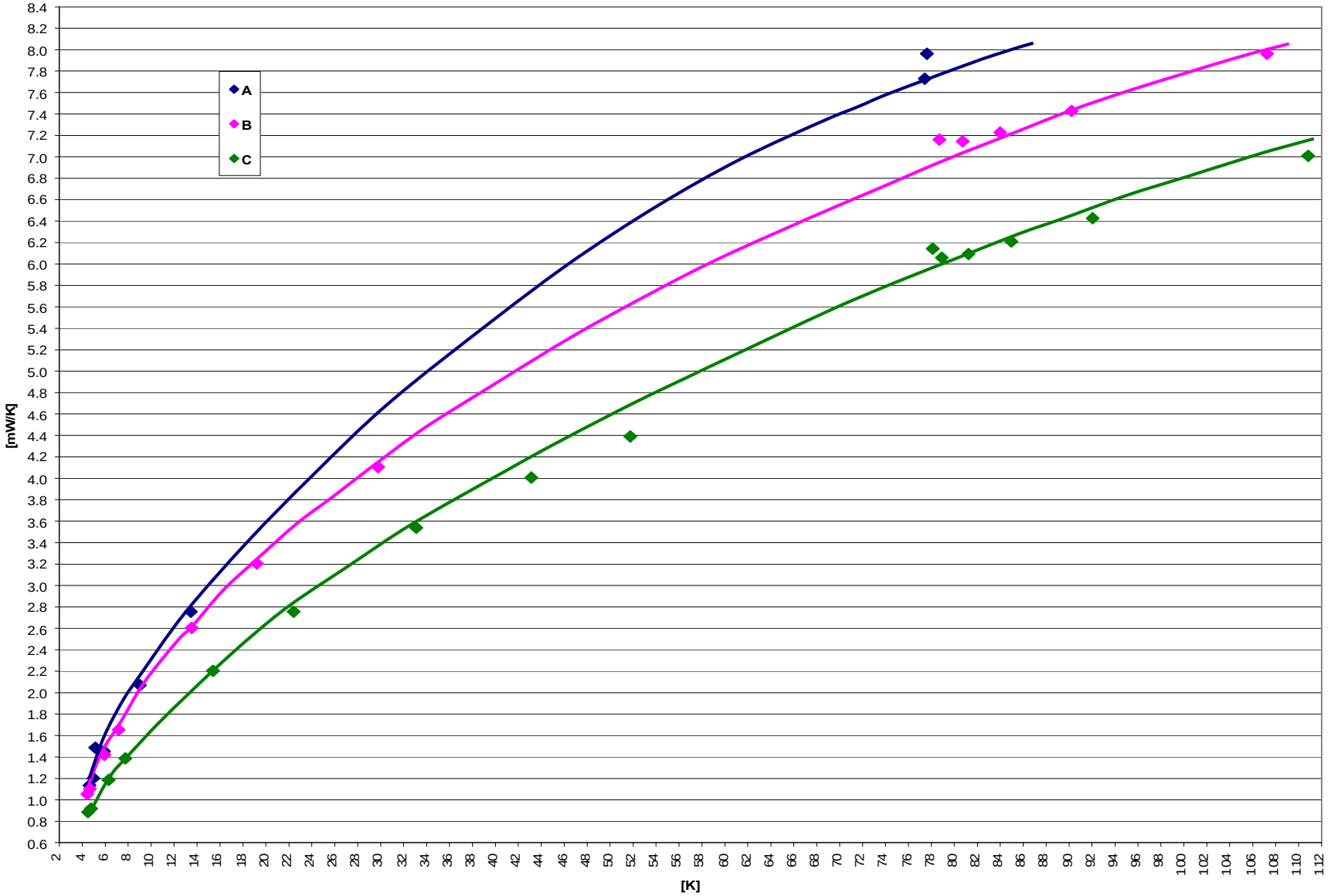

FIG. 15b: A, B, C, Sample Th. Conductance between TC1 – TC8

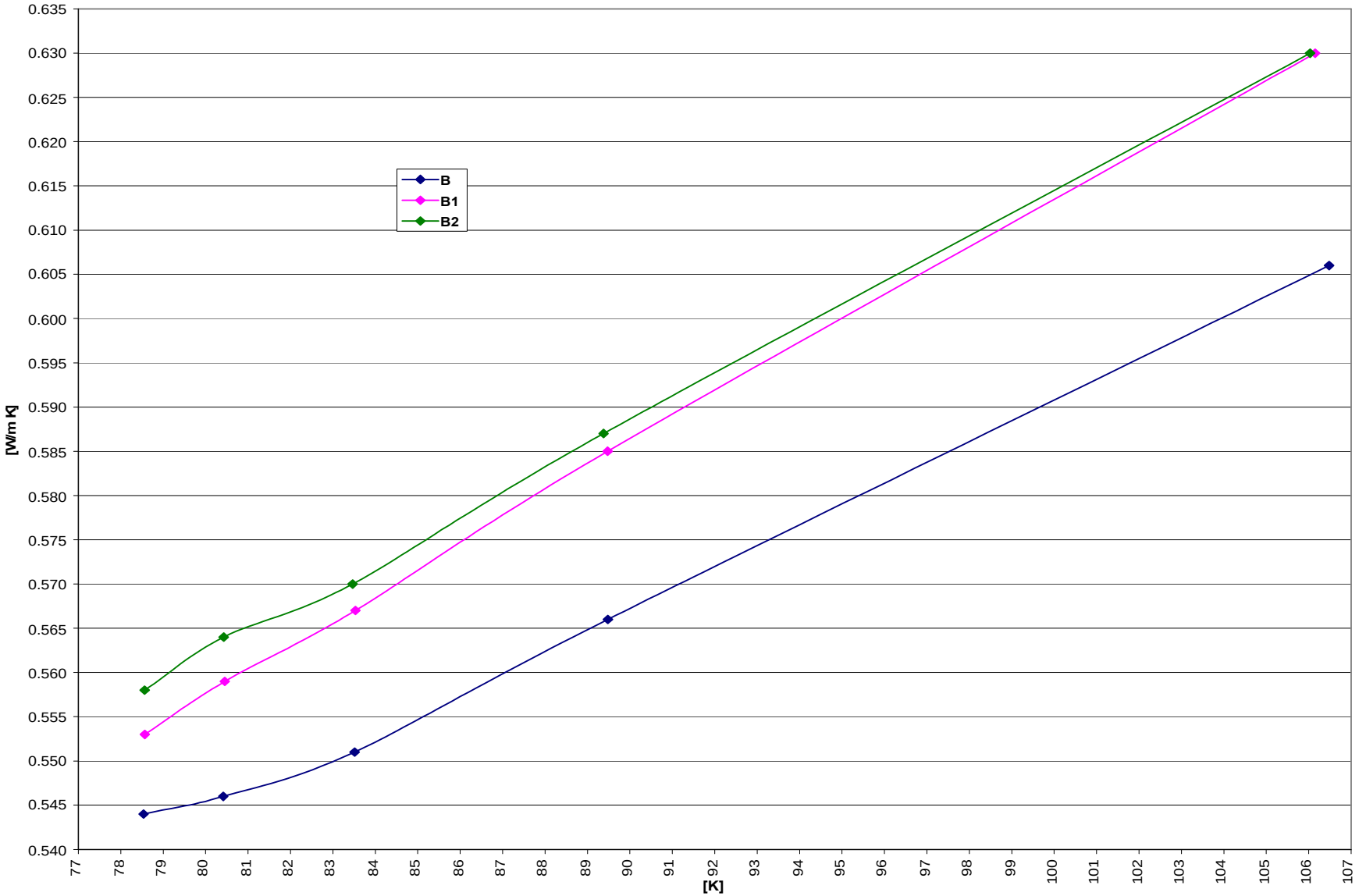

FIG. 16a: LN_2 B Sample Th. Conductivity between TC3 – TC7

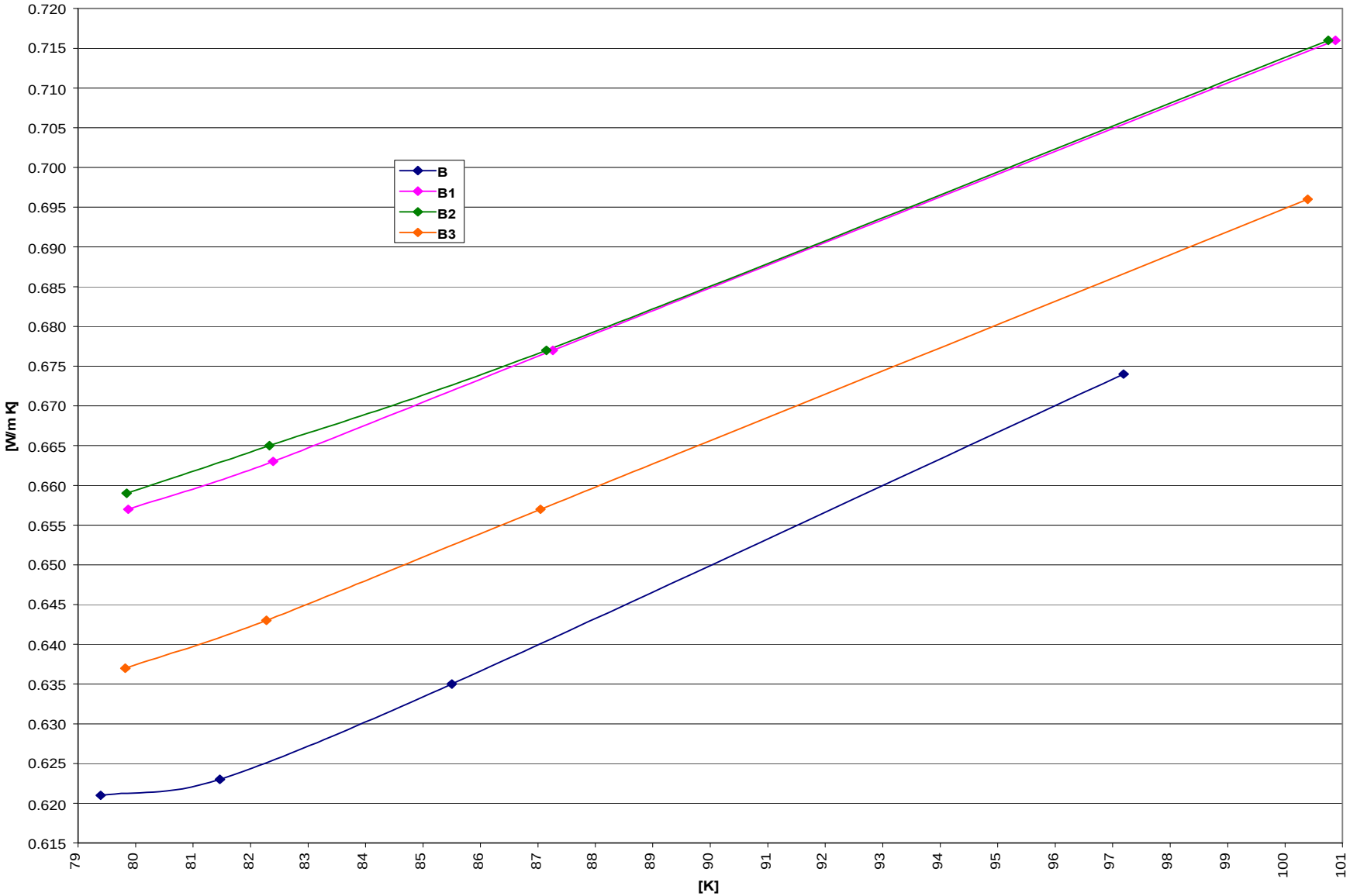

FIG. 16b: LN2 B Sample Th. Conductivity between TC2 – TC4

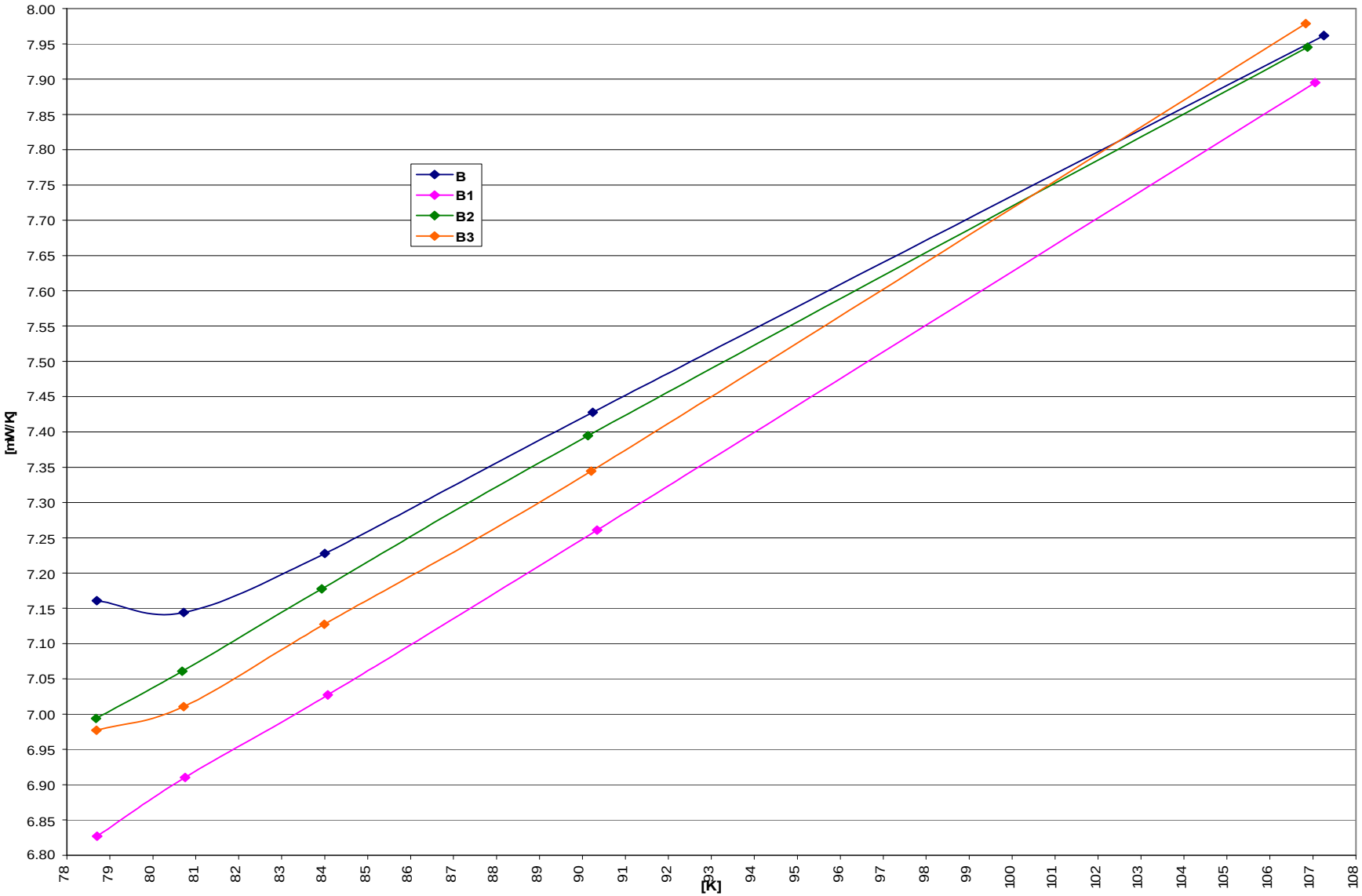

FIG. 16c: LN_2 B Sample Th. Conductance between TC1 – TC8

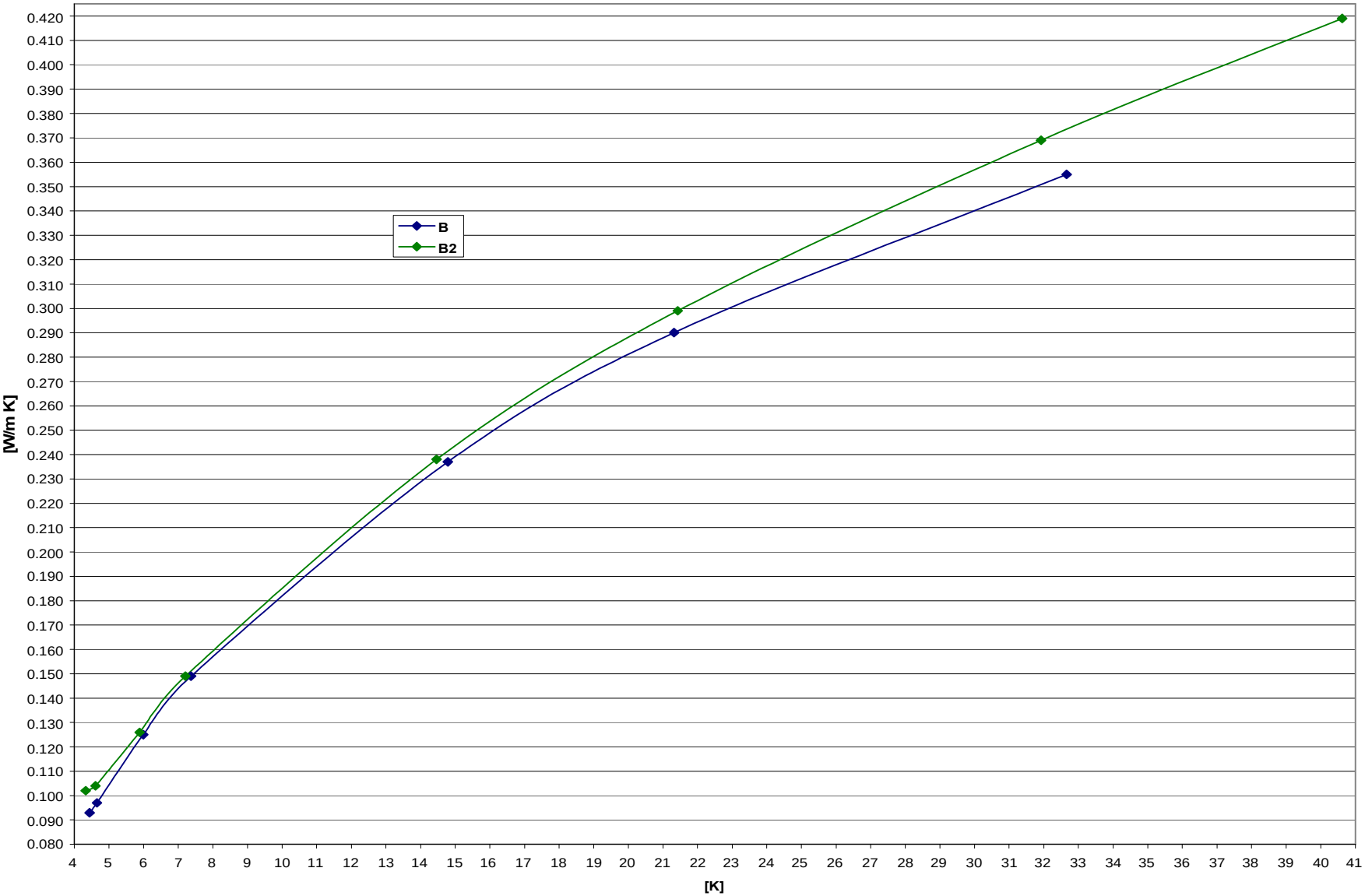

FIG. 17a: LHe B Sample Th. Conductivity between TC3 – TC7

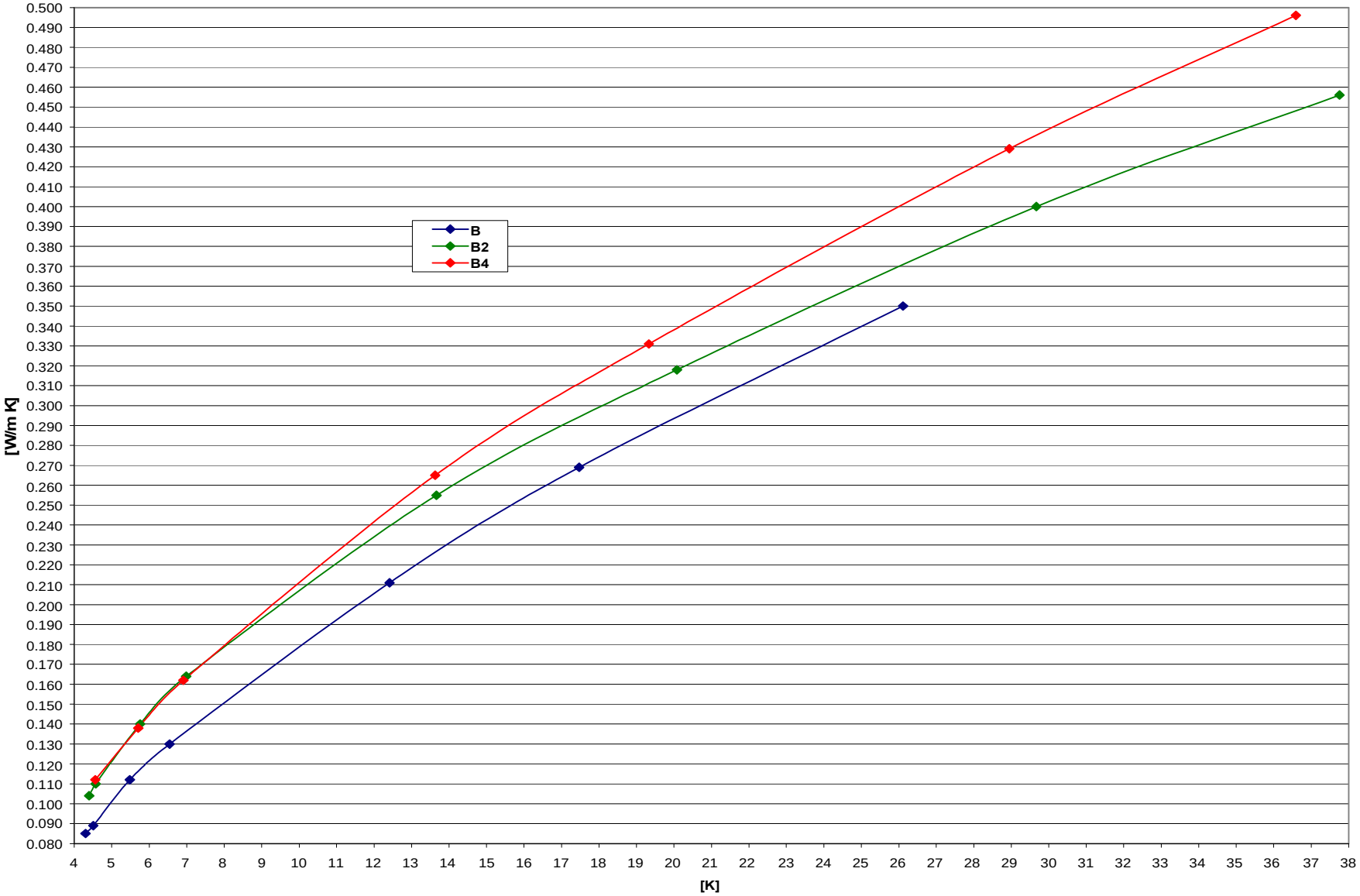

FIG. 17b: LHe B Sample Th. Conductivity between TC2 – TC4

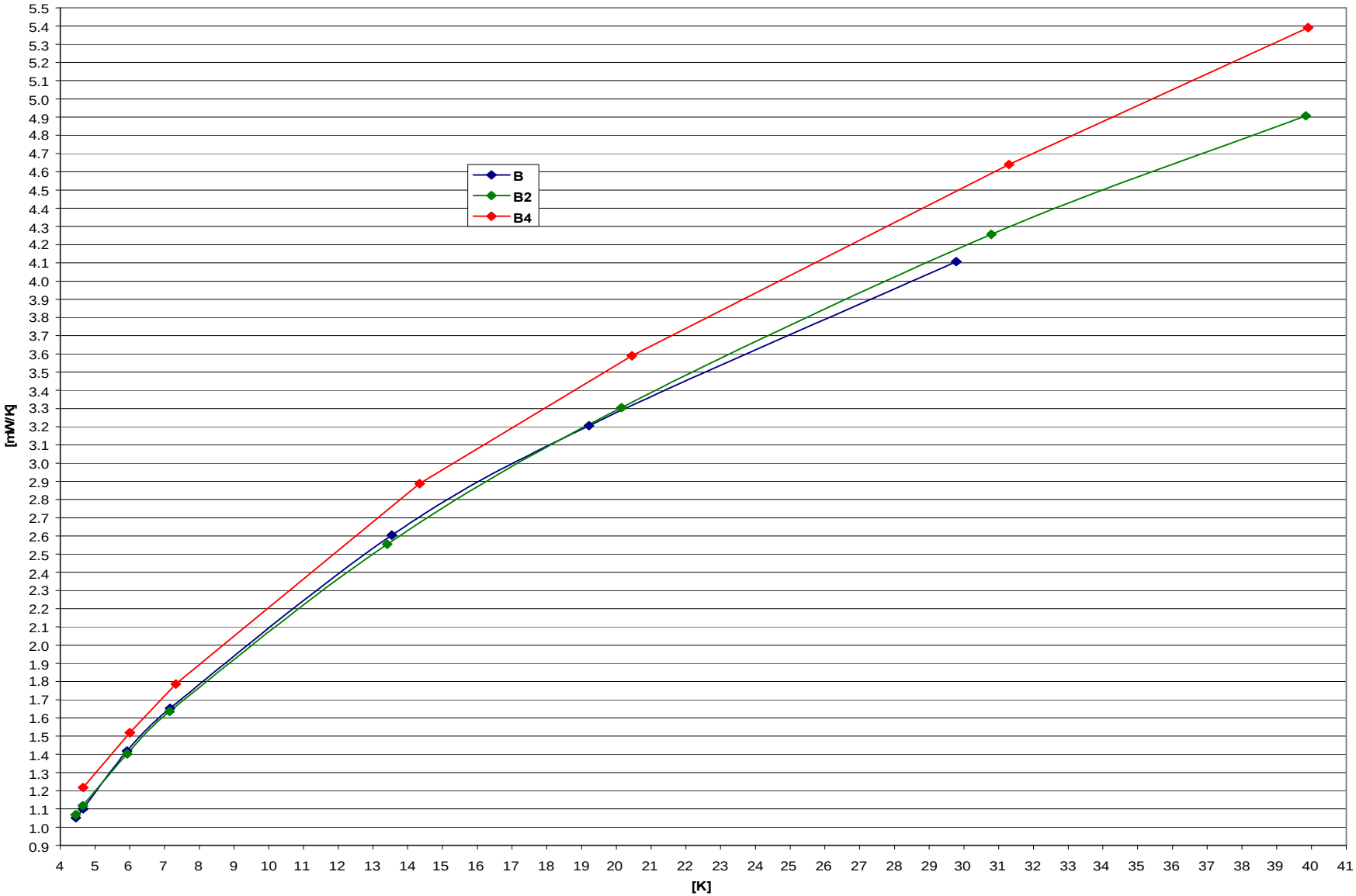

FIG. 17c: LHe B Sample Th. Conductance between TC1 – TC8

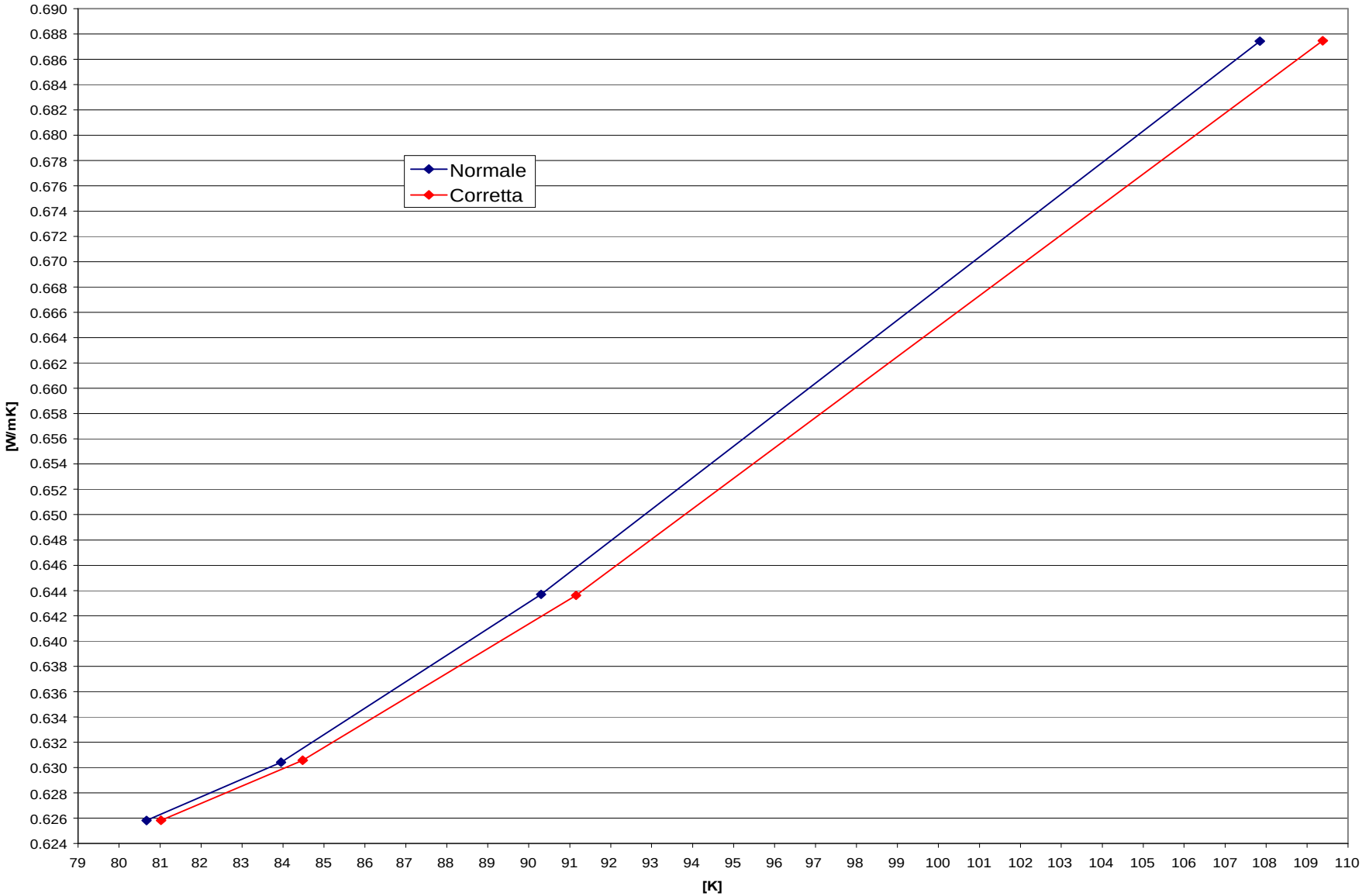

FIG 18a: C Sample: Isothermal Block Compensation to LN_2

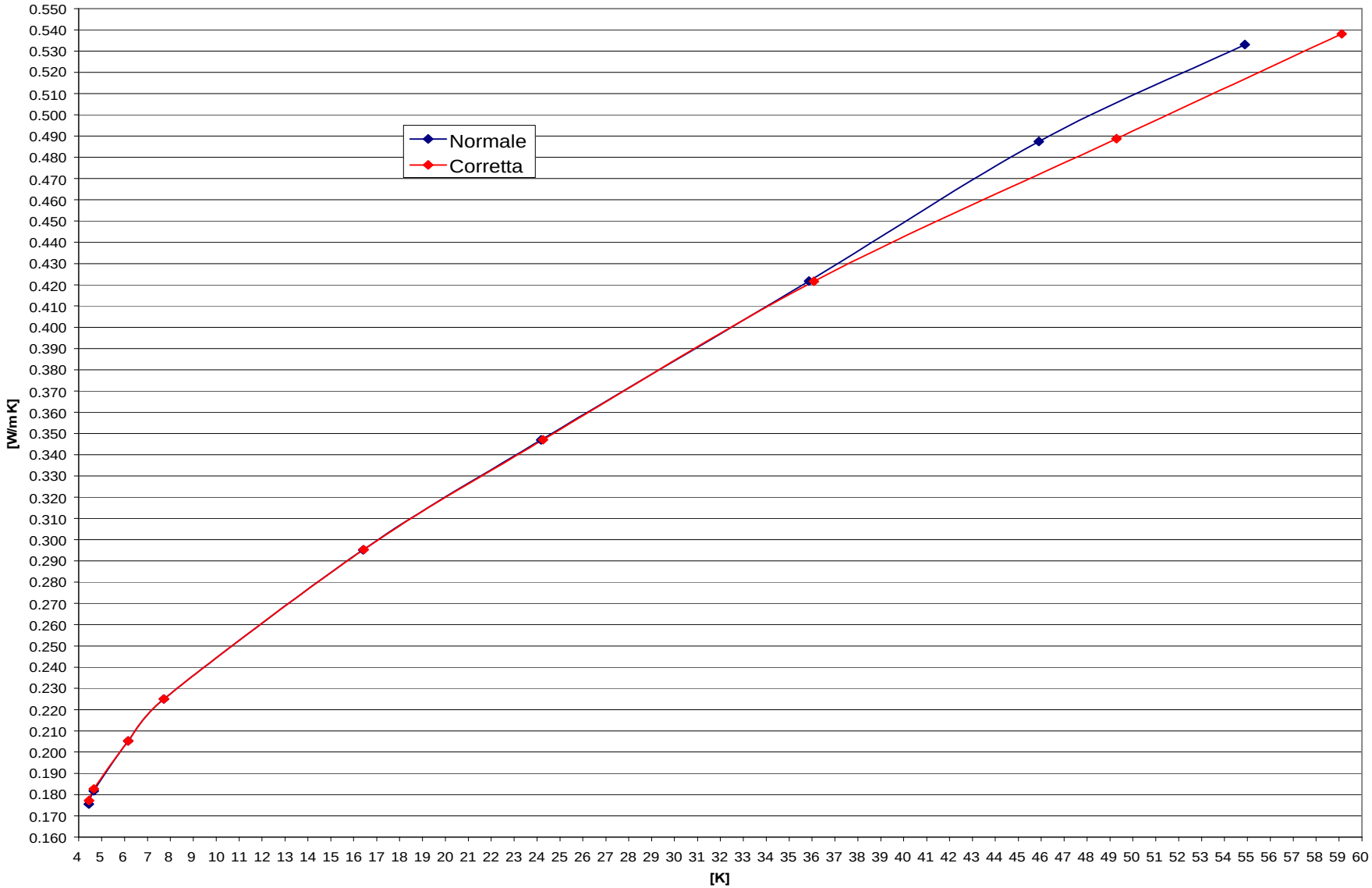

FIG 18b: C Sample: Isothermal Block Compensation to LHe